# Regulation of TRIB1 abundance in hepatoma models

Sébastien Soubeyrand, PhD[1]*, Paulina Lau MSc[1], and Ruth McPherson, MD, PhD [1,2]*.

[1] Atherogenomics Laboratory, University of Ottawa Heart Institute, Ottawa, Canada

[2] Division of Cardiology, Ruddy Canadian Cardiovascular Genetics Centre, University of Ottawa Heart Institute, Ottawa, Canada.

Short title: TRIB1 regulation in hepatoma models

* Correspondence:

ssoubeyrand@ottawaheart.ca

rmcpherson@ottawaheart.ca

## Abstract

Tribbles related homolog 1 (TRIB1) contributes to lipid and glucose homeostasis by facilitating the degradation of cognate cargos by the proteasome. We previously reported that TRIB1 was unstable in non-hepatic cellular models. Moreover, inclusion of proteasome inhibitors failed to prevent TRIB1 loss, consistent with the involvement of proteasome independent degradative processes. In view of the key role of TRIB1 in liver function, we continue our exploration of TRIB1 regulation pathways in two commonly used human hepatocyte models, HuH-7 and HepG2 cells. Proteasome inhibitors potently upregulated both endogenous and recombinant TRIB1 mRNA and protein levels. Increased transcript abundance was independent of MAPK activation while ER stress was a relatively mild inducer. Despite increasing TRIB1 protein abundance and stabilizing bulk ubiquitination, proteasome inhibition failed to stabilize TRIB1, pointing to the predominance of proteasome independent protein degradation processes controlling TRIB1 protein abundance in hepatomas. Proteasome inhibition via downregulation of its PSMB3 regulatory subunit, in contrast to its chemical inhibition, had minimal impact on TRIB1 levels. Moreover, immunoprecipitation experiments showed no evidence of TRIB1 ubiquitination. Cytoplasmic retained TRIB1 was unstable, indicating that TRIB1 lability is regulated prior to its nuclear import. Substitution of the TRIB1 PEST-like region with a GST helical region or N-terminal deletions failed to fully stabilize TRIB1. Finally, inclusion of protease or autophagy inhibitors *in vivo* did not rescue TRIB1 stability. This work excludes proteasome-mediated degradation as a significant contributor to TRIB1 instability and identifies transcriptional regulation as a

43 prominent mechanism regulating TRIB1 abundance in liver models in response to
44 proteasome inhibition.

## 45 Introduction

46 The TRIBBLES family comprises 3 evolutionary divergent forms in higher eukaryotes:
47 TRIB1, TRIB2 and TRIB3. A distinguishing feature is their ability to promote
48 degradation of cognate targets by enforcing their interaction with specific E3 ligases.
49 This functional network plays an important role in normal liver function by regulating lipid
50 metabolism but is also implicated in the development and progression of myeloblastic
51 leukemia [1–5]. Mammalian tribbles have also been shown to regulate MAPK
52 signaling in a coordinated fashion [4,6]. In D. Melanogaster, where a single Tribbles is
53 present, tribbles promotes rapid degradation of slbo turnover and ensures proper
54 oogenesis [7]. In addition, Tribbles inhibits cell cycle progression by facilitating String
55 and Twine proteasomal degradation [8] . Recently, the *TRIB1* gene locus has
56 renewed interest through its association with coronary artery disease (CAD). Although
57 it is still unclear whether *TRIB1* proper mediates the genetic association with CAD,
58 compelling evidence points to its role in lipid metabolism [5,9].

59 Tribbles are pseudokinases, namely proteins that lack phosphorylation activity
60 but leverage structural motifs shared by kinases [10]. Over the years, mammalian
61 *tribbles* have been shown to interact with several proteins. The best characterized
62 interaction is with the E3 ligase COnstitutively Photomorphogenic 1 (COP1). COP1 is a
63 RING finger E3 ligase, which in complex with E1 and E2 enzymes can catalyze
64 ubiquitination of target proteins, in some cases with the assistance of additional adaptor
65 proteins. By binding and recruiting CEBP to COP1, TRIB1 and TRIB2 enable

66 degradation of CEBPs [11–15]. While all 3 tribbles can constitutively interact with COP1
67 via their C-termini Val-Pro containing motif, only TRIB1 and TRIB2 target CEBP for
68 degradation, indicating that interaction might not be sufficient for degradation; by
69 contrast, all three can facilitate COP1 mediated ACC1 degradation when overexpressed
70 [1].

71 The fate of TRIB1 as an adaptor protein is unclear. E3 adaptor proteins,
72 including TRIB1, tend to be unstable [16]. Limited evidence however suggests that it
73 may not be degraded through the process of cargo degradation [17]. For TRIB3, COP1
74 overexpression reduces CEBPA without affecting TRIB3 levels, suggesting that TRIB3
75 is not degraded via COP1 [1]. Thus, TRIB1 may not be directly degraded by the
76 ubiquitin proteasome system (UPS). However the Val-Pro interface, mediating binding
77 of both adaptor proteins and targets to COP1, also plays a key role in earmarking
78 degradation targets (e.g. Jun, ATGL, ETS) [18,19].

79 Regulated protein degradation involves three major pathways. Removal of
80 ubiquitinated proteins typically occurs via the 26S, a large protein complex exhibiting 3
81 distinct protease activities [20–22]. Several proteasome inhibitors (PIs) have been
82 developed over the years, some of which have clinical implications [23,24]. Chief
83 among them is Velcade/Bortezomib (BTZ), used in the treatment of multiple myeloma.
84 Relevant to liver disease, BTZ therapy is sporadically linked to liver injury and has been
85 shown to exhibit hepatotoxicity in mouse models [25].

86 In addition to proteasome-mediated degradation, lysosomes and
87 autophagosomes also contribute to the removal of larger cargos via lysosomal
88 proteases [21,26]. All 3 pathways share some dependence on ubiquitination and are

89 likely functionally interconnected, particularly under stress [27]. For instance, interfering
90 with proteasome function can induce autophagy to help tackle the accumulation of
91 unwanted protein conjugates and contribute to homeostasis.

92 We previously demonstrated that TRIB1 regulation in non-liver models occurred
93 at multiple levels, involving proteasome dependent and independent processes at
94 transcriptional and post-transcriptional levels [28]. An intriguing finding was that
95 whereas drug mediated proteasome inhibition was sufficient to increase TRIB1 levels,
96 associated with increased transcription, proteasome inhibition was insufficient to
97 prevent loss of TRIB1 after CHX treatment, hinting to alternate pathways that could
98 degrade TRIB1. The current study examines the regulatory processes controlling TRIB1
99 abundance in greater detail, leveraging two commonly used human hepatocyte cell
100 models.

# 101 Materials and Methods

## 102 Cell culture and treatments

103 HuH-7 (Japanese Collection of Research Bioresources Cell Bank) and HepG2 (ATCC)
104 cells were maintained in physiological (5 mM) glucose DMEM media supplemented to
105 10% FBS and containing antimycin A and antibacterial supplements (Gibco). Drugs are
106 listed in the **Supplemental Material** section. Stable cell pools were obtained by 3 ug/ml
107 puromycin selection following viral transduction. Vehicle (DMSO or PBS) was added at
108 0.1% or less, final concentration.

109 ## Western blotting

110 Protein lysates (approximately 30 µl per lane) were resolved on 1.5 mm 8 % SDS-
111 PAGE gels unless mentioned otherwise and transferred to nitrocellulose membranes.
112 Membranes were blocked in Intercept buffer (LI-COR, 30 min), rinse briefly in PBS/0.1%
113 Tween (PBS/T) and incubation with the primary was typically performed in PBS/T for 16
114 h. Secondary antibodies were from Li-Cor (680 and 800) and were used as 1:20,000
115 dilutions. Antibody incubations were followed by one PBS/T and three PBS rinses. All
116 antibodies used are listed in the **Supplemental Material** section. TRIB1 is expressed at
117 very low levels and was undetectable in naïve HuH-7 and HepG2 using 2 distinct Abs
118 under basal conditions; lack of TRIB1 signal was ascertained using orthogonal
119 validation using antisense oligonucleotides and lack of responsiveness to actinomycin
120 D. Different lots of TRIB1 antibodies raised in rabbits (TRIB1r; targeting the N-terminal
121 region) were inconsistent in sensitivity but yielded comparable background signals.
122 The goat TRIB1 (TRIB1g) was more consistent across lots but exhibited slightly lower
123 sensitivity. Analyses were performed with either or both Ab as limited supplies
124 permitted. Endogenous and exogenous wild-type TRIB1 were detectable as a tight
125 band triplet with a prominent central band. Note that both Abs revealed the presence of
126 an overlapping non-specific band (resistant to TRIB1 siRNA and ACTD).

127 ## Immunoprecipitation

128 Whole cell lysates of HepG2-T1 (stably transduced with pLVXpuro-TRIB1) cells were
129 obtained by lysing cells in PBS containing 0.1% Triton X-100 (PBS/TX) as well as
130 protease and protein inhibitor cocktails (Roche) for 5 min on ice. Cleared lysates

131 (13,000 xg for 2 min @ 4 C) were adjusted to 1 mg/ml with PBS/TX buffer and
132 antibodies were added at 2 ug/mg lysate for 30 min, followed by the addition of protein
133 A/G beads (10 ul suspension; PureProteome, EMD Millipore) for an additional 5 h on an
134 orbital plate. Samples were then washed 4 X with 0.5 ml of IP buffer, heat denatured at
135 95 °C under reducing conditions (5 min) and analyzed by Western blot.

## 136 Real-Time RNA quantification (RT-qPCR)

137 RNA was extracted from culture plates using Tri Reagent (Roche) and isolated using
138 Direct-Zol RNA miniprep kits (Zymo Research). RNA was reverse transcribed using a
139 mixture of oligo dT and random hexamer primers (Roche). Quantification was
140 performed on a Light Cycler 480 using SYBR Green (Roche). Target of interest values
141 were expressed relative to the corresponding peptdidyl Peptidylprolyl Isomerase A
142 (PPIA) values using the $2^{-\Delta\Delta Ct}$ method. Oligonucleotides are listed in the
143 **Supplemental Material** section.

## 144 Plasmid and lentiviral constructs

145 TRIB1NES, wherein the bipartite TRIB1 nuclear localization sequence (AA 31-51) was
146 substituted for a PKIA nuclear export signal as described previously, was subcloned into
147 PLVX-puro [29]. For the PEST substituted construct, a synthetic fragment containing
148 the GST helical region, consisting of 2 identical helices, was used to replace the PEST
149 region (AA 53-88) of TRIB1 (see **Supplemental Material** section for sequence). N-
150 terminal truncated TRIB1 expression constructs (Δ2-51 and Δ2-91) were obtained by
151 sub-cloning TRIB1 from the corresponding pCFP-TRIB1 construct to pLVX via BamHI
152 transfer. Lentiviral constructs were packaged in 293FT cells using co-transfection of

153 pLVX constructs with with psPAX2 and pMD2.G (Addgene). Virus titers were estimated
154 using puromycin resistance in HEK-293T cells; an equivalent of 3 MOI was used per
155 infection.

156 **Microscopy**

157 Cells were seeded on glass coverslips and fixed with 4% PFA in PBS for 15 min and
158 subsequently permeabilized/fixed for 20 min in PBS containing 0.1% Triton X-100 and
159 5% FBS. Detection was performed by incubating with primary antibodies at 1:500
160 dilutions in PBS and secondaries (Jackson laboratories) at 1:2000 for 1 h in PBS/0.1%
161 Triton. Four 1-minute rinses in PBS were performed after each incubation. Cells were
162 mounted in Fluorescent Mounting Medium (DakoCytomation) supplemented with
163 Hoechst 33342. Microscopy was performed using a 63 X Oil Immersion lens on a Zeiss
164 Elyra microscope.

165 **Results**

166 **TRIB1 abundance in hepatocyte models is upregulated by**
167 **proteasome inhibitors**

168 In liver models, the PI bortezomib (BTZ) increased recombinant TRIB1 and
169 unexpectedly revealed a weak TRIB1 signal in vector transduced HepG2 (Fig 1A). The
170 presence of multiple novel bands was confirmed in naïve HepG2 but not in HuH-7 (Fig
171 1B). Moreover, as previously observed in non-liver models, TRIB1 was unstable, as
172 revealed by cycloheximide (CHX) treatment, resulting in the disappearance of the
173 TRIB1 signal within 5 h of the translation inhibitor (Fig 1B). Increased TRIB1 was
174 accompanied by a 3 to 14-fold TRIB1 transcript increase in HepG2 and HuH-7 cells,

175 respectively and was observed with other, mechanistically, and structurally distinct,
176 inhibitors Epoxomycine (EPOXO), Lactacystin (LACTA) (S1 Fig). With prolonged
177 incubation, TRIB1 was detected in both parental HepG2 and HuH-7 cells, indicating that
178 TRIB1 accumulates over time (Fig 2). Immunofluorescence revealed a weak TRIB1
179 reactive signal that was enriched in the nucleus following BTZ treatment, detectable
180 after as early as 5 h in HepG2 cells or after longer incubation in HuH-7(Fig 3, S2 Fig, S3
181 Fig).

182 *Fig 1. Overexpressed TRIB1 and endogenous TRIB1 are sensitive to CHX and*
183 *proteasome inhibition in HuH-7 and HepG2 cell models. A, PLVX and PLVX-TRIB1*
184 *stables were exposed to 5 h BTZ treatment in presence of CHX or vehicle (1% DMSO).*
185 *B, as in A, but parental HepG2 and HuH-7 were treated as indicated. Data*
186 *representative of 3 experiments. Quantifications (relative to TUBB) normalized to Mock*
187 *are shown.*

188 *Fig 2. Prolonged incubation with proteasome inhibitors reveals endogenous TRIB1 in*
189 *HepG2 and HuH-7 cells. A, TRIB1 in HuH-7 is increased in response to a 18 h*
190 *treatment with 2 μM epoxomicin (Epoxo) or 5 μM BTZ. Arrow indicates equivalent*
191 *position on both panels. Detection was performed either with goat or rabbit raised Abs*
192 *(in distinct channels), as indicated. B, Relative abundance in HepG2 and HuH-7 cells*
193 *following 18 h incubations with BTZ. Two different intensities are shown. Data are*
194 *representative of 3-5 experiments. Quantification is expressed relative toTUBB and*
195 *normalized to the Mock sample; for TRIB1 quantification, the TRIB1r signal was used.*

196 *Fig 3. Endogenous TRIB1 signal in HepG2 cells treated with BTZ treatment for 5 h.*
197 *HepG2 cells on coverslips were treated with BTZ (5 uM) for 5 h. Detection was*

198 *performed using a TRIB1 Ab (TRIB1g; red) and Hoechst (green) signal. Top,*
199 *representative overlay of signals from a group of cells. Bottom, individual channels of*
200 *highlighted nucleus. Image was smoothed with a Gaussian filter (default parameter*
201 *settings ZEN 3.3)*

## 202 Increased transcript abundance is the result of increased 203 transcription

204 Increased TRIB1 abundance could reflect increased transcript output or increased
205 stabilization. The role of transcription in regulating TRIB1 abundance in response to
206 BTZ was examined by blocking *de novo* POLII transcription with ACTD. Comparable
207 fold reductions in TRIB1 mRNA were observed upon treating control and BTZ treated
208 cells with ACTD, suggesting that ongoing transcription is required (Fig 4A). Moreover,
209 ACTD treatment was sufficient to prevent BTZ mediated protein accumulation (Fig 4B).

210 *Fig 4. Transcription inhibition blocks TRIB1 upregulation in response to 5 h BTZ*
211 *treatment. HuH-7 and HepG2 cells were treated with BTZ or vehicle (Veh), with and*
212 *without (Ctl) a preincubation with ACTD for 5 min. A, mRNA abundance in HuH-7 and*
213 *HepG2 cells. B, Western blot performed in HepG2 cells; endogenous protein signal was*
214 *undetectable in HuH-7 after 5 h. Within each cell type, differences between Ctl and*
215 *ACTD were highly significant ($p < 0.001$, one-way repeated measures ANOVA ).*

216

217 **Increased TRIB1 mRNA abundance in response to proteasome**

218 **inhibitors is independent of MAPK activation**

219 MAP kinases (p38, JNK and ERK1/2) are major regulators of cell proliferation and
220 stress response and may contribute to increased TRIB1 transcription in response to
221 BTZ induced proteotoxic stress. We previously demonstrated the essential role of
222 ERK1/2 in promoting TRIB1 transcription following mitochondrial stress in HepG2 cells
223 [30]. The contribution of ERK1/2 was tested by blocking of ERK1/2 activity with
224 PD98059; this however had no effect on the BTZ mediated increase in TRIB1 (Fig 5).
225 Proteasome inhibition also stabilizes and activates c-Jun via JNK; Jun is a major
226 component of AP-1 complex, which occupies the TRIB1 promoter in naïve HepG2 cells
227 and liver according to ENCODE data [31–33]. As for p38, it can be activated by
228 proteasome inhibition and has the potential to promote AP-1 function [34,35]. As
229 observed for ERK inhibition, inclusion of JNK and p38 inhibitors failed to block the BTZ
230 mediated increase in both HuH-7 and HepG2 cells. Finally combining all 3 had minimal
231 impact on TRIB1 upregulation by BTZ. Thus increased TRIB1 mRNA abundance does
232 not require the contribution of MAPKs.

233 *Fig 5. BTZ mediated increased mRNA abundance is independent of MAPK activity.*
234 *HuH-7 and HepG2 cells were treated with BTZ for 5 h in the presence of MAPK*
235 *inhibitors (PD: PD98059 (ERK1/2) , SB: SB203580 (P38) , SP: SP600125 (JNK)), either*
236 *singly or in combination, as indicated; Ctl cells were treated with vehicle only (1%*
237 *DMSO). Individual biological replicates are shown (± SEM). TRIB1 expression is*
238 *normalized to PPIA levels. Differences between [MAPKi + BTZ] treatments and BTZ*

239 *were not statistically significant (one-way repeated measures ANOVA with Dunn's post-*
240 *hoc test vs Ctl).*

## 241 TRIB1 levels are weakly responsive to ER stress

242 Proteasome inhibition, by interfering with protein turnover of misfolded proteins
243 targeted for secretion, has the potential to induce ER stress and an unfolded protein
244 response (UPR). Interestingly TRIB3 has been shown to be highly responsive to ER
245 stress induction via tunicamycin in HepG2 cells [36]. Indeed, BTZ treatment elicited a
246 stress response as assessed by increased CHOP and BiP in both HCC cell lines (S4
247 Fig). To examine the potential of ER stress in controlling TRIB1 levels, cells were
248 treated with tunicamycin, a prototypical ER stress inducer. A 5 h (or 22 h) tunicamycin
249 increased TRIB1 abundance modestly (1.1-2-fold); by comparison, tunicamycin
250 treatment resulted in a 5 to 20-fold BiP and CHOP increase in both hepatoma models
251 (Fig 6). Together, these findings indicate that ER stress occurs in response to BTZ in
252 hepatoma models but that it is insufficient to singly account for the 4 to 15-fold
253 increased TRIB1 mRNA levels elicited by PI treatments in HepG2 and HuH-7.

254 *Fig 6. ER stress is a weak TRIB1 inducer. HuH-7 and HepG2 cells were treated with*
255 *Tunicamycin (12 μM) for either 5 or 18 h (O/N). Bars represent the means +/- S/D. *,*
256 *p<0.05, ** p< 0.01 from Vehicle. Paired Student t-test, Tunica vs vehicle.*

## 257 Upregulation of TRIB1 by proteasome inhibitors is rapid and is
## 258 dependent on increased transcription

259 A time course was performed to better characterize the upregulation at the protein level.
260 To visualize TRIB1 at early time points, when endogenous protein abundance is too low

261 for detection, the assay was performed on recombinant TRIB1. To address possible
262 off-target BTZ effects on non-proteasome proteases [37], lactacystin (LACTA), a
263 structurally and mechanistically distinct inhibitor was also used [23]. Lactacystin was
264 included at a concentration previously shown to inhibit ~70% of the proteasome
265 chymotryptic activity *in situ* [38]. Rapid TRIB1 upregulation was detectable within 1 h
266 of treatment using both BTZ and LACTA and increased over 5 h (Fig 7). As observed
267 above with the endogenous transcript, PIs potently upregulated recombinant TRIB1
268 mRNA (S5 Fig).

269 *Fig 7. Upregulation of recTRIB1 by proteasome inhibitors is rapid. Western blot*
270 *analyses of time course experiments. Stable pools of HuH-7-T1 and HepG2-T1 cells*
271 *were treated for 1 to 5 h with BTZ (5 μM) (A) or LACTA 10 μ M (B) for the indicated*
272 *time. Samples were resolved by Western blot and analyzed with the indicated*
273 *antibodies.*

274 Increased protein abundance could be the result of increased transcript reduced
275 protein degradation, increased transcription, increased translation, or a combination
276 thereof. Upregulation was blocked by ACTD, as noted earlier with the endogenous
277 protein, indicating that increased recombinant TRIB1 protein abundance requires
278 transcription (Fig 8).

279 *Fig 8. Increased recTRIB1 following proteasome inhibition is blocked by ACTD. HuH-7*
280 *and HepG2 cells stably expressing TRIB1 were incubated for 5 h with lactamycin*
281 *(LACTA,10 μM) and/or Actinomycin D (ACTD, 5 μg/ml)), as indicated. Data*
282 *representative of 3 experiments. Quantifications represent TUBB normalized signal*
283 *intensity, expressed relative to the corresponding Ctl values*.

284 **The proteasome plays a limited role in the control of steady state**

285 **TRIB1**

286 Evidence to date points to the major contribution of transcription in regulating TRIB1
287 abundance when the proteasome is blocked. These experiments however were
288 performed in the presence of inhibitors with unavoidable off-target effects. To address
289 these limitations, the proteasome regulatory beta 3 subunit (PSMB3) was targeted by
290 siRNA. Reduced *PSMB3* expression resulted in increased abundance of coupled
291 ubiquitin chains, consistent with impaired proteasome function allowing ubiquitinated
292 proteins to accumulate. The treatment was however insufficient to reveal endogenous
293 TRIB1 protein signal (Fig 9A). Lack of detection could be due to absent or insufficient
294 protein upregulation. To distinguish between these 2 scenarios, proteasome inhibition
295 via PSMB3 was repeated on cells expressing the ~ 10-20-fold more abundant
296 recombinant *TRIB1*. Reduced PSMB3 levels were associated with a subtle increase in
297 TRIB1, which reached statistical significance only in HepG2-T1 (1.2-fold ± 0.07; n=3)
298 and could be due to a correlative 1-5-2-fold increased TRIB1 mRNA (Fig 9B; S6 Fig).

299 *Fig 9. Long term proteasome suppression increases polyUb but has minimal impact on*
300 *TRIB1 abundance. Western blot analyses of PSMB3 silenced samples. A, B: HuH-7*
301 *and HepG2 cells (with or without transduced TRIB1, as indicated) were treated 96 h*
302 *with siRNA targeting PSMB3 or a siRNA control. C, For Ub, region spanning 100 kDa to*
303 *the top of the gel is shown. Arrow points to the predicted position of TRIB1.*
304 *Quantification represents the TUBB corrected TRIB1 levels, normalized to the NT*
305 *control value*.

306

## 307 No evidence of TRIB1 ubiquitination using overexpression 308 approaches

309 Evidence of TRIB1 ubiquitination was tested by performing immunoprecipitation under
310 both basal and proteasome blocked conditions. Independent of drug treatment, no
311 detectable ubiquitin was associated with TRIB1. With the limitation that protein
312 ubiquitination may not always be required for proteasome-mediate degradation (e.g.
313 [39]), these results further support the contribution of non-proteasome mediated
314 degradation processes (Fig 10).

315 *Fig 10. Immunoprecipitated TRIB1 shows no evidence of ubiquitination. HepG2-T1*
316 *cells, treated with either BTZ or vehicle (0.25% DMSO) for 5 h were immunoprecipitated*
317 *with either TRIB1g or COL4A1 goat polyclonal antibodies and analyzed by Western*
318 *blotting using rabbit anti-Ub (top) or anti-TRIB1 (bottom). Detection was sequential (Ub*
319 *then TRIB1r). * indicates a non-specific (likely IgG related) band.*

## 320 TRIB1 loss upon CHX occurs more rapidly than bulk ubiquitin

321 The mechanisms triggering the loss of TRIB1 protein were then investigated. First, loss
322 of TRIB1 and bulk ubiquitination in the presence of BTZ were compared. Whereas
323 TRIB1 loss in response to CHX was pronounced, loss of coupled Ub was minimal over
324 5 h (~23% and ~ 13% signal loss in HepG2 and HuH-7, respectively), consistent with
325 extensive proteasome inhibition and suggesting that the mechanisms responsible for
326 TRIB1 and bulk ubiquitination removal are distinct (Fig 11).

327 *Fig 11. Loss of polyUb in response to CHX is slower compared to TRIB1 in the*
328 *presence of BTZ. Western blot analysis of HuH7-T1 and HepG2-T1 treated with the*
329 *indicated drugs for 5 h. A, representative Western blots. Levels of polyUb were*
330 *quantified over the 100-150 kDa range. B, Relative sensitivities of TRIB1 and polyUb*
331 *signals to BTZ and CHX after a 5 h treatment. Quantifications of the TRIB1 signals and*
332 *polyUb (TUBB corrected) in HepG2-T1 and HuH-7-T1 cells following BTZ and/or CHX*
333 *treatments. Dashed line indicates a no-loss scenario. Average of 3 independent*
334 *experiments. *, p < 0.05; **, p<0.01; Unpaired T-test, TRIB1 vs ConjUb.*

## 335 High dose of Carfilzomib or proteasome inhibitor cocktails do not
## 336 prevent TRIB1 loss to CHX

337 The proteasome contains three distinct activities with different sensitivities to PI
338 classes. Indeed, BTZ preferentially targets the chymotrypsin-like and caspase-like
339 activities of the proteasome over the trypsin-like activity. Thus, CHX mediated loss of
340 TRIB1 upon PI treatments may reflect incomplete inhibition of the proteasome, possibly
341 with preferential engagement of the tryptic activity. Carfilzomib is an irreversible,
342 clinically relevant, epoxyketone inhibitor that blocks trypsin-like and chymotrypsin-like
343 activities at high doses *in situ* [40]. Inclusion of Carfilzomib had no impact on TRIB1 loss
344 however (S7A Fig). To further exclude a proteasome contribution, a combination
345 approach was undertaken next. Combined PI use has been shown to increase
346 inhibition potency, possibly reflecting allosteric facilitation [40]. HepG2-T1 cells were
347 incubated in the presence of 3 mechanistically distinct inhibitors: BTZ, LACTA and
348 EPOXO. Combining, all 3 inhibitors did not curb TRIB1 loss however, further
349 minimizing the likelihood of proteasome implication (S7B Fig).

350 **Proteasome suppression via PSMB3 silencing fails to prevent TRIB1**
351 **loss to CHX**

352 A putative contribution of the proteasome machinery to TRIB1 degradation under
353 chemical inhibition was further tested by examining TRIB1 loss to CHX after PSMB3
354 silencing and PI cocktail; we reasoned that PSMB3 silencing may reveal putative
355 inhibitor resistant residual proteasome activity. As demonstrated earlier (Fig. 9),
356 *PSMB3* silencing was associated with increased bulk protein ubiquitination, indicating
357 impaired proteasome function, yet did not help stabilize TRIB1 in the presence both
358 BTZ and CHX (Fig 12).

359 *Fig 12. Proteasome-silencing fails to prevent TRIB1 loss to CHX. Western blot*
360 *analyses of PSMB3-silenced HepG2-T1 cells. HepG2-T1 cells were treated 96 h with*
361 *siRNA targeting PSMB3 or a siRNA control. During the last 5 h, cells were pre-treated*
362 *for 5 min with BTZ, followed by the inclusion of CHX for 5 h. For polyUb, region*
363 *spanning 75 kDa to the top of the gel is displayed. Quantification of the TRIB1g/TUBB*
364 *signals (normalized to NT1si) is shown.*

365 **COP1 does not regulate TRIB1 protein abundance and turnover**

366 COP1 is an E3 ligase functionally integrated, albeit not exclusively, with TRIB1. It
367 normally resides in both nuclear and cytoplasmic compartments and can shuttle
368 between the 2 compartments [41]. To test whether COP1 plays a role in the loss of
369 TRIB1 in the presence of CHX (under conditions where the proteasome is functional), a
370 TRIB1 construct deficient in COP1 binding, as well as a Wild-type version for direct

371 comparison, were transduced in HepG2 [42]. Both variants were similarly sensitive to
372 CHX, demonstrating TRIB1 instability does not require COP1 interaction (Fig 13).

373 *Fig 13. COP1 binding interface is not required for TRIB1 instability. Stable pools of*
374 *HepG2 cells transduced with either Wt or VP-AA variants were treated with BTZ and/or*
375 *CHX as indicated for 5 h. Cell lysates were then analyzed by Western blotting using*
376 *TRIB1 (rabbit) and TUBB antibodies. Data is representative of 2 biologicals.*
377 *Quantifications are internally controlled to the matching TUBB signal and are expressed*
378 *relative to the Ctl HepG2-T1.*

## 379 Instability of TRIB1 does not require the The Pro-Glu-Ser-Thr (PEST) 380 region or the N-terminal region of TRIB1

381 The N-terminal region of TRIB2 was implicated in mediating its instability [43]. TRIB1
382 contains a predicted disordered N-terminus (https://mobidb.bio.unipd.it/Q96RU8;
383 Alphafold) that is enriched in P, E, S and T residues, reminiscent of PEST domains
384 associated with protein instability [44]. To examine whether the PEST-like region played
385 a role in destabilizing TRIB1, we substituted the domain for 2 amphipathic helices of
386 equivalent lengths derived from the more stable GST protein. The substituted TRIB1
387 was potently upregulated by BTZ but remained highly unstable to CHX, implying that
388 the PEST region is not necessary to confer TRIB1 instability (Fig 14). Similar
389 conclusions were drawn from N-terminal truncations: deletion of either AA 2-51 or AA 2-
390 91 of TRIB1 did not render TRIB1 resistant to CHX (Fig 14). Interestingly, the latter
391 deletion constructs did not show the cluster of bands typical of full-length TRIB1, hinting
392 that this feature is dictated by its N-terminal region and is unrelated to its instability.

393 *Fig 14. Substitution of TRIB1 PEST region with a GST helical region or N-terminal*
394 *deletions fail to stabilize TRIB1. A, approximately to-scale schematic of the deletions.*
395 *B, C, Western blot analysis of stable pools of HepG2 and HuH7 cells expressing TRIB1*
396 *with PEST to GST domain substitutions (dPEST) or harboring N-terminal deletions were*
397 *treated as indicated with CHX and/or BTZ for 5 h. In C, Top, HuH-7-ΔT1; bottom,*
398 *HepG2- ΔT1 cells. Experiment was repeated twice with similar results.*

## 399 Cytosolically retained TRIB1 is unstable

400 TRIB1 instability could result from regulatory events taking place early during TRIB1
401 synthesis in the cytosol or after its nuclear import. To test the relative contribution of
402 cytosolic and nuclear processes, we took advantage of a TRIB1 construct wherein the
403 bipartite nuclear localization sequence was replaced PKIA nuclear export signal. We
404 previously showed using transient transfection that TRIB1 was unstable in HeLa cells.
405 To mitigate issues noted previously relating to the greater stability of transiently
406 transfected TRIB1, TRIB1 was transduced by lentiviral delivery. As previously
407 described in non-hepatic cell models, the protein localized exclusively to the cytoplasm
408 (S8 Fig). Inclusion of BTZ resulted in its upregulation, although substituted TRIB1
409 (TRIB1dNLS) was increased only 2-fold vs ~4- to 8-fold, for Wt TRIB1 in HepG2 and
410 HuH-7, respectively (Fig 15). Importantly, upon CHX addition, TRIB1 was rapidly lost,
411 in line with degradation processes occurring in the cytosol prior to its nuclear import.

412 *Fig 15. Cytosol-retained TRIB1 is upregulated by BTZ and is sensitive to CHX. Stable*
413 *pools of TRIB1NES expressing cells generated in HepG2 and HuH-7 cells. Cells were*
414 *treated for 5 h with BTZ in the presence or absence of CHX. Data are representative of*
415 *3 independent experiments.*

416 **TRIB1 proteolysis occurs independently of the lysosomal system and**

417 **is resistant to protease inhibitors *in vivo***

418 The lysosomal proteolytic machinery uses its own set of proteases and is largely
419 independent of the proteasome, at least under normal conditions. Proteasome
420 inhibition however was shown previously to activate the lysosomal-autophagy which we
421 hypothesized could be responsible for TRIB1 degradation; this would be consistent with
422 our evidence of cytoplasmic TRIB1 degradation [45]. A possible contribution of the
423 lysosome was tested using CLQ, an inhibitor of lysosome acidification, which is required
424 to activate resident proteases. Prolonged incubation of HepG2-T1 with CLQ, which
425 increased LC3BII, an indicator of lysosome-autophagy inhibition, failed however to
426 prevent recombinant TRIB1 loss (Fig 16). Moreover, basal TRIB1 was not affected by
427 CLQ, which has been previously shown to impair proteasome function (albeit in
428 fibroblasts), further ruling against a contribution of the UPS to TRIB1 degradation [46]

429 *Fig 16. Autophagy inhibition does not impact TRIB1 instability. Western blot analysis of*
430 *HepG2-T1 cells incubated for 24 h in the presence of CLQ (5 μM) to block autophagy.*
431 *BTZ and CHX were added during the last 5 h of incubation. LC3B and TRIB1r samples*
432 *were resolved on 8% and 15% gels, respectively. Experiment was repeated twice with*
433 *similar results.*

434 Lastly, the contributions of putative proteases were tested by inhibitor screens in
435 HepG2-T1 cells in the presence of BTZ. Broad specificity compounds targeting the
436 major classes of proteases (Ser, Cys and Asp proteases) were selected. Inclusion of
437 cell-permeant protease inhibitors targeting Serine (Pefabloc/AEBSF), Cysteine (E64

438 and TPCK) and Aspartic acid proteases (Pepstatin A) as well as Calpains (CALPi) and
439 Caspases (ZVAD-FMK) failed to prevent TRIB1 loss resulting from CHX treatment (S9
440 Fig).

## 441 Discussion

442 Here we characterized TRIB1 accumulation by proteasome inhibition in hepatocyte
443 models. We show this to be accompanied by increased transcription, as well as
444 instability under proteasome permissive and non-permissive conditions. TRIB1
445 abundance was strongly increased, largely through transcriptional upregulation but
446 remained unstable in the hepatocyte models examined. This differs from our previous
447 work using non hepatocyte models, wherein we reported a more limited contribution of
448 transcript upregulation (i.e. insensitivity to ACTD) in controlling TRIB1 protein levels
449 following BTZ treatment [29]. We hypothesize that this in part stems from greater
450 TRIB1 mRNA stability, rendering the protein steady state levels less sensitive to ACTD.
451 Importantly TRIB1 remained highly sensitive to CHX in the presence of BTZ, indicating
452 that proteasome-independent protein instability is conserved in all models examined to
453 date.

454 A possible confounder is the ability of cells to detoxify and/or rapidly export non-
455 covalent inhibitors (e.g BTZ). However, the incubation conditions (relatively short,
456 continuous and in the presence of high concentrations), combined with very slow off
457 rates (for BTZ at least [47]) should minimize these possibilities. Moreover, stability of
458 the poly-Ub signal observed in the presence of PIs indicates that proteasome inhibition
459 is persistent. Although it cannot be totally excluded that low, residual activity is sufficient
460 to degrade TRIB1, a lack of proteasome involvement in TRIB1 degradation is further

461 supported by the absence of identifiable Ub-TRIB1 complexes, with the caveat that Ub-
462 TRIB1 abundance may be too low to detect. Absence of Ub signal does not exclude a
463 proteasome contribution however: the 20S proteasome, which lacks the gatekeeper
464 19S regulatory particle responsible for ubiquitin recognition, can promote degradation of
465 ubiquitinated targets [48,49].

466 The proteasome is responsible for the vast majority of protein degradation,
467 including most short lived proteins [50]. Co-translational degradation via the UPS is
468 widespread and contributes to protein synthesis quality control [51–54]. It has been
469 estimated that 12-15% of nascent polypeptides are ubiquitinated in HEK293T [51]. In
470 that case, in contrast to TRIB1, de novo co-translated proteins are ubiquitinated and can
471 be readily stabilized by proteasome inhibition. Non UPS proteolytic pathways,
472 sometimes detectable only in the absence of functional proteasome, have been
473 described, including Calpains, TPP2 and others (e.g. [55–59]). According to the
474 MEROPS database, the human proteome contains 703 putative and validated
475 proteases, most of which await elucidation of biological role and might function in more
476 specialized forms of intracellular proteolysis.

477 In contrast to TRIB1, TRIB2 has been shown to be subjected to ubiquitination via
478 smuf1 and/or bTRCP, and possibly proteasome-mediated degradation, although this
479 remains to be formally tested via an inhibitor approach [43,60]. Thus, despite their
480 shared origins, divergent regulatory mechanisms may have co-evolved to regulate
481 individual tribbles. Indeed, while TRIB2 instability to CHX treatment (when
482 overexpressed in HE293T) was largely abrogated by removal of its disordered N-
483 terminal 50 AA, TRIB1 deletions spanning the N-terminus as well as substitutions of AA

484 31 to 88 (NLS + PEST regions) were insufficient to stabilize TRIB1. In addition, TRIB2
485 can be destabilized pharmacologically via an interaction between its pseudo kinase
486 domain and a family of EGFR inhibitors [61]. As all tribbles proteins harbor somewhat
487 conserved pseudo kinase domain, this domain may render TRIB1 unstable. Instability
488 could be mediated via post-translation modifications (PTMs). For instance, for both
489 cyclin D1 and AKT, phosphorylation impairs (proteasome-mediated) degradation
490 [54,62]. Relatively little is known about TRIB1 PTMs. TRIB1 migration on SDS-PAGE,
491 characterized by several closely migrating bands, is certainly consistent with low
492 molecular weight covalent modifications (e.g., phosphorylation). Interestingly, an
493 analogous pattern was observed with terminal the PEST- and NLS-substituted TRIB1
494 (AA 53-88 and AA 30-51, respectively) construct but not with the Δ2-51 N-terminal
495 deletion, implying that this pattern requires AA 2-29 of TRIB1.

496 While we present evidence excluding possible degradative pathways, the how
497 and why of TRIB1 instability remain unknown. Recognition subunits of E3 ligase, like
498 TRIB1, tend to be rapidly turned over, suggesting that instability is functionally important
499 [16]. Interestingly, TRIB1 instability appears independent of its interaction with COP1,
500 as suggested by the propensity of the binding deficient variant to remain unstable.
501 Rapid TRIB1 turn over might stem from quality control events, perhaps to address a
502 propensity of TRIB1 to misfold. Alternatively, TRIB1 may be specifically turned over to
503 ensure a timely adaptation to changing cellular conditions. Given the role of TRIB1 in
504 cell growth and proliferation, one could envision interactors either stabilizing or
505 destabilizing the emerging TRIB1 to match nutrient abundance. Future work will
506 explore these possibilities.

## Acknowledgments

This work was funded by a Canadian Institutes for Health Research Foundation grant (FRN:154308; RM).

510 # References


511 **1**. Dedhia PH, Keeshan K, Uljon S, Xu L, Vega ME, Shestova O, et al. Differential
512 ability of Tribbles family members to promote degradation of C/EBPalpha and
513 induce acute myelogenous leukemia. Blood. 2010;116: 1321–8.

514 **2**. Burkhardt R, Toh SA, Lagor WR, Birkeland A, Levin M, Li X, et al. Trib1 is a lipid-
515 and myocardial infarction–associated gene that regulates hepatic lipogenesis and
516 VLDL production in mice. J Clin Invest. 2010;120: 4410–4414.

517 **3**. Yoshino S, Yokoyama T, Sunami Y, Takahara T, Nakamura A, Yamazaki Y, et al.
518 Trib1 promotes acute myeloid leukemia progression by modulating the
519 transcriptional programs of Hoxa9. Blood. 2021;137: 75–88.

520 **4**. Yokoyama T, Kanno Y, Yamazaki Y, Takahara T, Miyata S, Nakamura T. Trib1
521 links the MEK1/ERK pathway in myeloid leukemogenesis . Blood . 2010;116:
522 2768–2775.

523 **5**. KY H, RC B. Competing tissue-specific functions for the Tribbles-1 plasma lipid
524 associated locus. Curr Opin Lipidol. 2021;32: 175–182.

525 **6**. Guan H, Shuaib A, Leon DD De, Angyal A, Salazar M, Velasco G, et al.
526 Competition between members of the tribbles pseudokinase protein family shapes
527 their interactions with mitogen activated protein kinase pathways. Sci Rep.
528 2016;6: 32667.

529 **7**. Rorth P, Szabo K, Texido G. The level of C/EBP protein is critical for cell
530 migration during Drosophila oogenesis and is tightly controlled by regulated
531 degradation. Mol Cell . 2000;6: 23–30.

532 **8**. Mata J, Curado S, Ephrussi A, Rorth P. Tribbles coordinates mitosis and
533 morphogenesis in Drosophila by regulating string/CDC25 proteolysis. Cell.
534 2000;101: 511–522.

535 **9**. Johnston JM, Angyal A, Bauer RC, Hamby S, Kim Suvarna S, Baidžajevas K, et
536 al. Myeloid Tribbles 1 induces early atherosclerosis via enhanced foam cell
537 expansion. Sci Adv. 2019;5.

538 **10**. Mace PD, Murphy JM. There's more to death than life: Noncatalytic functions in
539 kinase and pseudokinase signaling. J Biol Chem. Elsevier; 2021;296.

540 **11**. Keeshan K, He Y, Wouters BJ, Shestova O, Xu L, Sai H, et al. Tribbles homolog 2
541 inactivates C/EBPα and causes acute myelogenous leukemia. Cancer Cell.
542 2006;10: 401–411.

543 **12**. Naiki T, Saijou E, Miyaoka Y, Sekine K, Miyajima A. TRB2, a mouse Tribbles
544 ortholog, suppresses adipocyte differentiation by inhibiting AKT and C/EBPbeta. J
545 Biol Chem. 2007;282: 24075–82.

546 **13**. Yamamoto M, Uematsu S, Okamoto T, Matsuura Y, Sato S, Kumar H, et al.
547 Enhanced TLR-mediated NF-IL6 dependent gene expression by Trib1 deficiency .
548 J Exp Med . 2007;204: 2233–2239.

549 **14**. Yoshida A, Kato JY, Nakamae I, Yoneda-Kato N. COP1 targets C/EBPα for
550 degradation and induces acute myeloid leukemia via Trib1. Blood. 2013;122:
551 1750–1760.

552 **15**. Wang X, Tokheim C, Gu SS, Wang B, Tang Q, Li Y, et al. In vivo CRISPR

553 screens identify the E3 ligase Cop1 as a modulator of macrophage infiltration and
554 cancer immunotherapy target. Cell. Elsevier; 2021;184: 5357-5374.e22.

555 **16**. Li J, Cai Z, Vaites LP, Shen N, Mitchell DC, Huttlin EL, et al. Proteome-wide
556 mapping of short-lived proteins in human cells. Mol Cell. Cell Press; 2021;81:
557 4722-4735.e5.

558 **17**. Ito H, Nakamae I, Kato J, Yoneda-Kato N. Stabilization of fatty acid synthesis
559 enzyme acetyl-CoA carboxylase 1 suppresses acute myeloid leukemia
560 development. J Clin Invest. 2021;131.

561 **18**. Lu G, Zhang Q, Huang Y, Song J, Tomaino R, Ehrenberger T, et al.
562 Phosphorylation of ETS1 by src family kinases prevents its recognition by the
563 COP1 tumor suppressor. Cancer Cell. 2014;26: 222–234.

564 **19**. Ghosh M, Niyogi S, Bhattacharyya M, Adak M, Nayak DK, Chakrabarti S, et al.
565 Ubiquitin Ligase COP1 controls hepatic fat metabolism by targeting ATGL for
566 degradation. Diabetes. 2016;65: 3561–3572.

567 **20**. Navon A, Ciechanover A. The 26 S Proteasome: From Basic Mechanisms to Drug
568 Targeting. J Biol Chem. 2009;284: 33713–33718.

569 **21**. Dikic I. Proteasomal and Autophagic Degradation Systems. Annu Rev Biochem.
570 2017;86: 193–224.

571 **22**. Collins GA, Goldberg AL. The Logic of the 26S Proteasome. Cell. 2017;169: 792–
572 806.

573 **23**. Ōmura S, Crump A. Lactacystin: first-in-class proteasome inhibitor still excelling

574 and an exemplar for future antibiotic research. J Antibiot (Tokyo).2019;72: 189–
575 201.

576 **24**. Harer SL, Bhatia MS, Bhatia NM. Proteasome inhibitors mechanism; source for
577 design of newer therapeutic agents. J Antibiot. 2012;65: 279–288.

578 **25**. Mutluay D, Monsef YA, Tenekeci GY. Evaluation of Potential Hepatotoxicity
579 Induced by Bortezomib. Acta Sci Vet. Universidade Federal do Rio Grande do
580 Sul; 2021;49: 1826.

581 **26**. Shaid S, Brandts CH, Serve H, Dikic I. Ubiquitination and selective autophagy .
582 Cell Death Differ . Macmillan Publishers Limited ; 2013;20: 21–30. Available:
583 http://dx.doi.org/10.1038/cdd.2012.72

584 **27**. Rusilowicz-Jones E V., Urbé S, Clague MJ. Protein degradation on the global
585 scale. Mol Cell. Elsevier; 2022;82: 1414–1423.

586 **28**. Turner AW, Martinuk A, Silva A, Lau P, Nikpay M, Eriksson P, et al. Functional
587 analysis of a novel genome-wide association study signal in SMAD3 that confers
588 protection from coronary artery disease. Arterioscler Thromb Vasc Biol. 2016;36:
589 972–983.

590 **29**. Soubeyrand S, Martinuk A, Lau P, McPherson R. TRIB1 is regulated post-
591 transcriptionally by proteasomal and non-proteasomal pathways. PLoS One.
592 2016;11.

593 **30**. Soubeyrand S, Naing T, Martinuk A, McPherson R. ERK1/2 regulates hepatocyte
594 Trib1 in response to mitochondrial dysfunction. Biochim Biophys Acta. 2013;1833:

595 3405–14.

596 **31**. Davis CA, Hitz BC, Sloan CA, Chan ET, Davidson JM, Gabdank I, et al. The
597 Encyclopedia of DNA elements (ENCODE): data portal update. Nucleic Acids
598 Res. 2018;46: D794–D801.

599 **32**. Dunham I, Kundaje A, Aldred SF, Collins PJ, Davis CA, Doyle F, et al. An
600 integrated encyclopedia of DNA elements in the human genome. Nature.
601 2012;489: 57–74.

602 **33**. Nakayama K, Furusu A, Xu Q, Konta T, Kitamura M. Unexpected Transcriptional
603 Induction of Monocyte Chemoattractant Protein 1 by Proteasome Inhibition:
604 Involvement of the c-Jun N-Terminal Kinase-Activator Protein 1 Pathway. J
605 Immunol. 2001;167: 1145–1150.

606 **34**. Wu WT, Chi KH, Ho FM, Tsao WC, Lin WW. Proteasome inhibitors up-regulate
607 haem oxygenase-1 gene expression: requirement of p38 MAPK (mitogen-
608 activated protein kinase) activation but not of NF-kappaB (nuclear factor kappaB)
609 inhibition. Biochem J. 2004;379: 587–593.

610 **35**. Herlaar E, Brown Z. p38 MAPK signalling cascades in inflammatory disease. Mol
611 Med Today. 1999;5: 439–447.

612 **36**. Ohoka N, Yoshii S, Hattori T, Onozaki K, Hayashi H. TRB3, a novel ER stress-
613 inducible gene, is induced via ATF4-CHOP pathway and is involved in cell death .
614 EMBO J . 2005;24: 1243–1255.

615 **37**. Arastu-Kapur S, Anderl JL, Kraus M, Parlati F, Shenk KD, Lee SJ, et al.

616 Nonproteasomal targets of the proteasome inhibitors bortezomib and carfilzomib:
617 A link to clinical adverse events. Clin Cancer Res. 2011;17: 2734–2743.

618 **38**. Csizmadia V, Csizmadia E, Silverman L, Simpson C, Raczynski A, O'Brien L, et
619 al. Effect of proteasome inhibitors with different chemical structures on the
620 ubiquitin-proteasome system in vitro. Vet Pathol. 2010;47: 358–367.

621 **39**. Gomard T, Jariel-Encontre I, Basbous J, Bossis G, Mocquet-Torcy G, Piechaczyk
622 M. Fos family protein degradation by the proteasome. Biochem Soc Trans.
623 2008;36: 858–863.

624 **40**. Besse A, Besse L, Kraus M, Mendez-Lopez M, Bader J, Xin BT, et al.
625 Proteasome Inhibition in Multiple Myeloma: Head-to-Head Comparison of
626 Currently Available Proteasome Inhibitors. Cell Chem Biol. 2019;26: 340-351.e3.

627 **41**. Kung JE, Jura N. The pseudokinase TRIB 1 toggles an intramolecular switch to
628 regulate COP 1 nuclear export . EMBO J. 2019;38.

629 **42**. Qi L. TRB3 Links the E3 Ubiquitin Ligase COP1 to Lipid Metabolism. Science
630 2006;312: 1763–1766.

631 **43**. Wang J, Zhang Y, Weng W, Qiao Y, Ma L, Xiao W, et al. Impaired
632 phosphorylation and ubiquitination by p70 S6 kinase (p70S6K) and Smad
633 ubiquitination regulatory factor 1 (Smurf1) promote tribbles homolog 2 (TRIB2)
634 stability and carcinogenic property in liver cancer . J Biol Chem. 2013;288:
635 33667–33681.

636 **44**. Mészáros B, Kumar M, Gibson TJ, Uyar B, Dosztányi Z. Degrons in cancer. Sci

637 Signal. 2017;10.

638 **45**. Zhu K, Dunner K, McConkey DJ. Proteasome inhibitors activate autophagy as a
639 cytoprotective response in human prostate cancer cells. Oncogene. 2010;29:
640 451–462.

641 **46**. Myeku N, Figueiredo-Pereira ME. Dynamics of the degradation of ubiquitinated
642 proteins by proteasomes and autophagy: Association with sequestosome 1/p62. J
643 Biol Chem. 2011;286: 22426–22440.

644 **47**. Kisselev AF, Van Der Linden WA, Overkleeft HS. Proteasome Inhibitors: An
645 Expanding Army Attacking a Unique Target. Chem Biol. 2012;19: 99–115.

646 **48**. Waku T, Nakamura N, Koji M, Watanabe H, Katoh H, Tatsumi C, et al. NRF3-
647 POMP-20S Proteasome Assembly Axis Promotes Cancer Development via
648 Ubiquitin-Independent Proteolysis of p53 and Retinoblastoma Protein. Mol Cell
649 Biol. 2020;40: e00597-19.

650 **49**. Orlowski M, Wilk S. Ubiquitin-independent proteolytic functions of the
651 proteasome. Arch Biochem Biophys. 2003;415: 1–5.

652 **50**. Pajonk F, McBride WH. The Proteasome in Cancer Biology and Treatment.
653 Radiat Res. 2001;156: 447–459.

654 **51**. Wang F, Durfee LA, Huibregtse JM. A Cotranslational Ubiquitination Pathway for
655 Quality Control of Misfolded Proteins. Mol Cell. 2013;50: 368–378.

656 **52**. Gandin V, Topisirovic I. Co-translational mechanisms of quality control of newly
657 synthesized polypeptides. Translation. 2014;2: e28109.

658 **53**. Lykke-Andersen J, Bennett EJ. Quality control: Protecting the proteome:
659 Eukaryotic cotranslational quality control pathways. J Cell Biol. 2014;204: 467–
660 476.

661 **54**. Oh WJ, Wu CC, Kim SJ, Facchinetti V, Julien LA, Finlan M, et al. mTORC2 can
662 associate with ribosomes to promote cotranslational phosphorylation and stability
663 of nascent Akt polypeptide. EMBO J. 2010;29: 3939–3951.

664 **55**. Wang X, Wang F, Sy MS, Ma J. Calpain and other cytosolic proteases can
665 contribute to the degradation of retro-translocated prion protein in the cytosol. J
666 Biol Chem. J Biol Chem; 2005;280: 317–325.

667 **56**. Wang Y, Zhang Y. Regulation of TET Protein Stability by Calpains. Cell Rep.
668 2014;6: 278–284.

669 **57**. Chang AHK, Jeong J, Levine RL. Iron regulatory protein 2 turnover through a
670 nonproteasomal pathway. J Biol Chem. 2011;286: 23698–23707.

671 **58**. Tomkinson B. Tripeptidyl-peptidase II: Update on an oldie that still counts.
672 Biochimie. 2019;166: 27–37.

673 **59**. Acquaviva C, Salvat C, Brockly F, Bossis G, Ferrara P, Piechaczyk M, et al.
674 Cellular and viral Fos proteins are degraded by different proteolytic systems.
675 Oncogene 2001 208. 2001;20: 942–950.

676 **60**. Qiao Y, Zhang Y, Wang J. Ubiquitin E3 ligase SCF(beta-TRCP) regulates TRIB2
677 stability in liver cancer cells. Biochem Biophys Res Commun. 2013;441: 555–559.

678 **61**. Foulkes DM, Byrne DP, Yeung W, Shrestha S, Bailey FP, Ferries S, et al.

679 Covalent inhibitors of EGFR family protein kinases induce degradation of human
680 Tribbles 2 (TRIB2) pseudokinase in cancer cells. Sci Signal. American
681 Association for the Advancement of Science; 2018;11: eaat7951.

682 **62**. Diehl JA, Zindy F, Sherr CJ. Inhibition of cyclin D1 phosphorylation on threonine-
683 286 prevents its rapid degradation via the ubiquitin-proteasome pathway. Genes
684 Dev. 1997;11: 957–972.

685

686

687 # Supporting information captions

688 S1 Fig. TRIB1 mRNA increases in response to proteasome inhibitors in HuH-7 and
689 HepG2 cells. TRIB1 mRNA abundance (normalized to PPIA level) was measured
690 following 5 h regimen with the indicated drugs. Values are expressed relative to the
691 vehicle (1 % DMSO). Data represent the average of 3 experiments ± S.D. All changes
692 from vehicle (except for LACTA 2 μM; HepG2) were statistically significant ($p<0.05$)

693 S2 Fig. Endogenous TRIB1 signal is specific, nuclear and is detectable in HepG2 cells
694 following a 5 h BTZ treatment. HepG2 cells were seeded on coverslips and treated as
695 indicated with BTZ (5 μM) and/or CHX (10 μg/ml). Cells were then fixed and
696 permeabilized prior to incubations with either a TRIB1 antibody (1:500, +) or no antibody
697 (-) for 1 h. Cells were then washed and incubated for 1 h with a Donkey anti-goat
698 (DAG633) secondary Ab (1:2000) and counterstained with Hoechst. Images were
699 smoothed with a Gaussian filter.

700 S3 Fig. Increased TRIB1g reactive nuclear signal in HuH-7 treated for 18 h with BTZ 5
701 μM. A, wide field (60 X). CARS2 is included as a cytoplasmic marker. B, magnification
702 of yellow boxed region shown on left, smoothed with Gauss filter processing. TRIB1g
703 (peudocolored red), Hoechst's (pseudocolored lime green).

704 S4 Fig. BTZ induces changes consistent with the establishment of an ER stress
705 response in HepG2 and HuH-7 cells. Treatment with BTZ (5 h) increases BiP and
706 CHOP mRNA levels. Values were first normalized to PPIA and are expressed relative
707 to vehicle (1% DMSO). Paired Student t-test, BTZ vs vehicle. *, $P<0.05$; **; $P<0.01$

708 S5 Fig. Increased recTRIB1 upon proteasome treatment. HuH-7 and HepG2 cells
709 stably expressing TRIB1 were incubated with vehicle (Ctl), LACTA, BTZ or EPOXO at
710 the indicated concentrations for 5 h. A, protein abundance assessed by Western blot; B,
711 mRNA abundance as measured by qRT-PCR Data representative of 2 experiments.

712 S6 Fig. PSMB3 suppression leads to increased TRIB1 mRNA abundance in HepG2-T1
713 but not HuH7-T1 cells. PSMB3 was suppressed for 72 h and mRNA abundance was
714 measured by qRT-PCR. mRNA levels were corrected for PPIA and are expressed
715 relative to a non-specific control (NT).

716 S7 Fig. High doses carfilzomib or a proteasome inhibitor cocktail does not prevent
717 TRIB1 loss to CHX in HepG2-T1 cells. Western blot analyses of HepG2-T1 cells
718 treated with proteasome inhibitors. In A, HepG2-T1 cells were treated with the indicated
719 carfilzomib, either alone or in the presence of CHX for 5 h; carfilzomib was added 5 min
720 prior to CHX (10 μg/ml). In B, cells were treated for 5 h with a 5 min preincubation with
721 BTZ (B), vehicle (Ctl, 1% DMSO) or a combination of BTZ (B, 5 μM), Lactacystin (L, 10
722 μm) and Epoxomicin (E, 2 μm) and/or with 10 μg/ml cycloheximide (CHX), where
723 indicated. Experiments were repeated twice with similar results. Quantifications are the
724 TUBB-corrected TRIB1 signal and are normalized to the Ctl value (B) or the matching
725 CHX-free value (A). Experiments were repeated twice, with similar results.

726 S8 Fig. TRIB1NES expression in transduced HuH-7 and HepG2. HuH-7 and HepG2
727 cells stably transduced with TRIB1NES were treated for 5 h with BTZ. Fixed cells were
728 permeabilized and incubated for 16 h with TRIB1g antibody. T1g was detected with an
729 Alexa 633 donkey anti-goat Ab . Nuclei were counterstained with Hoechst.

730 S9 Fig. Preincubation with protease inhibitors cannot prevent TRIB1 loss in the
731 presence of CHX and BTZ. HepG2-T1 cells were treated with BTZ in the presence of
732 PEFABLOC (PEFA, 200 μM), Pepstatin A (PEPA, 1 μM), E64 (2 μM), calpain inhibitor 1
733 (CALPi, 20 μM), ZVAD-FMK (ZVAD, 1 μM) and TPCK (25 μM). Protease inhibitors were
734 added concurrently with BTZ and 5 min prior to the addition of CHX. Data are
735 representative of 3 experiments.

736

737

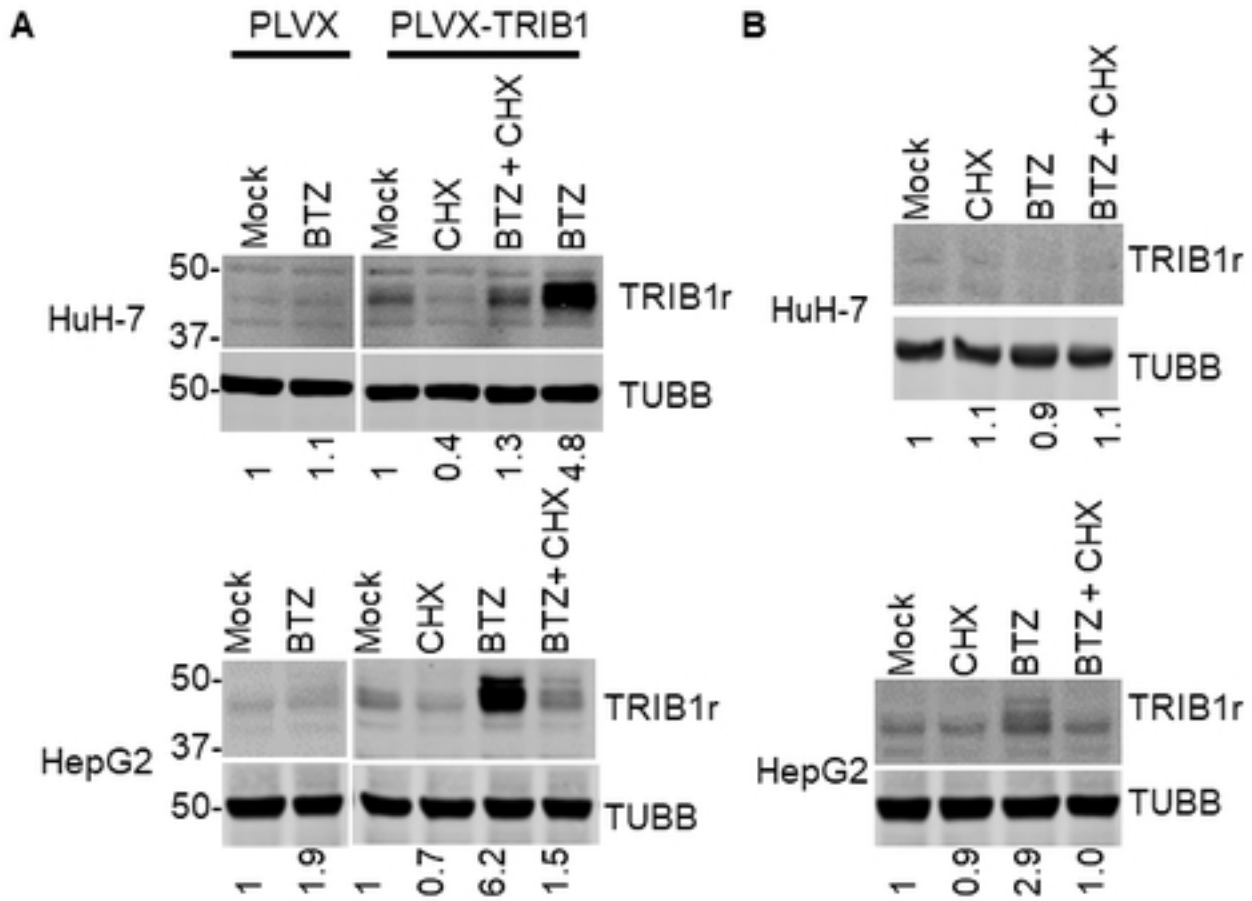
A
PLVX
PLVX-TRIB1
Mock
BTZ
Mock
CHX
BTZ + CHX
BTZ
HuH-7
50-
37-
50-
TRIB1r
TUBB
1
1.1
1
0.4
1.3
4.8
Mock
BTZ
Mock
CHX
BTZ
BTZ+ CHX
HepG2
50-
37-
50-
TRIB1r
TUBB
1
1.9
1
0.7
6.2
1.5
B
Mock
CHX
BTZ
BTZ + CHX
HuH-7
TRIB1r
TUBB
1
1.1
0.9
1.1
Mock
CHX
BTZ
BTZ + CHX
HepG2
TRIB1r
TUBB
1
0.9
2.9
1.0

figure 1

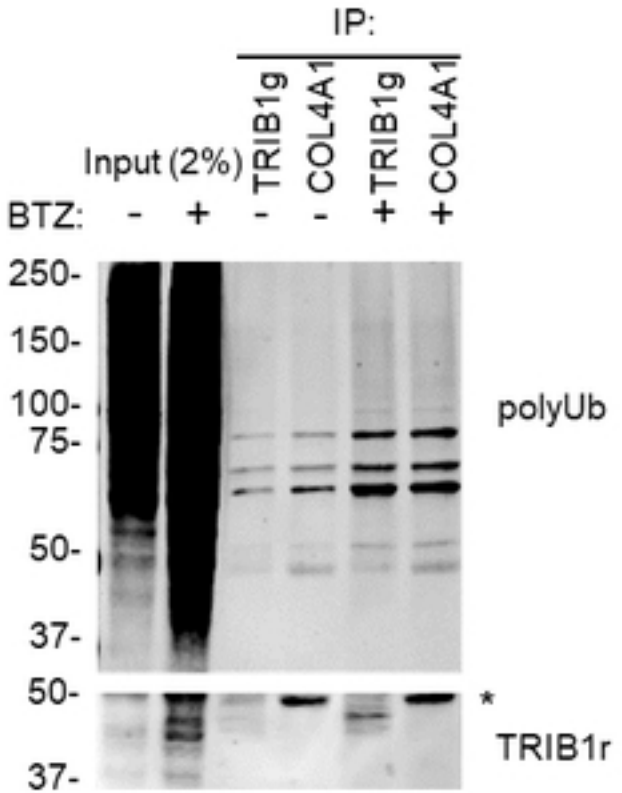
IP:
Input (2%)
- TRIB1g
- COL4A1
+ TRIB1g
+ COL4A1
BTZ:
-
+
250-
150-
100-
75-
50-
37-
polyUb
50-
37-
*
TRIB1r

figure 10

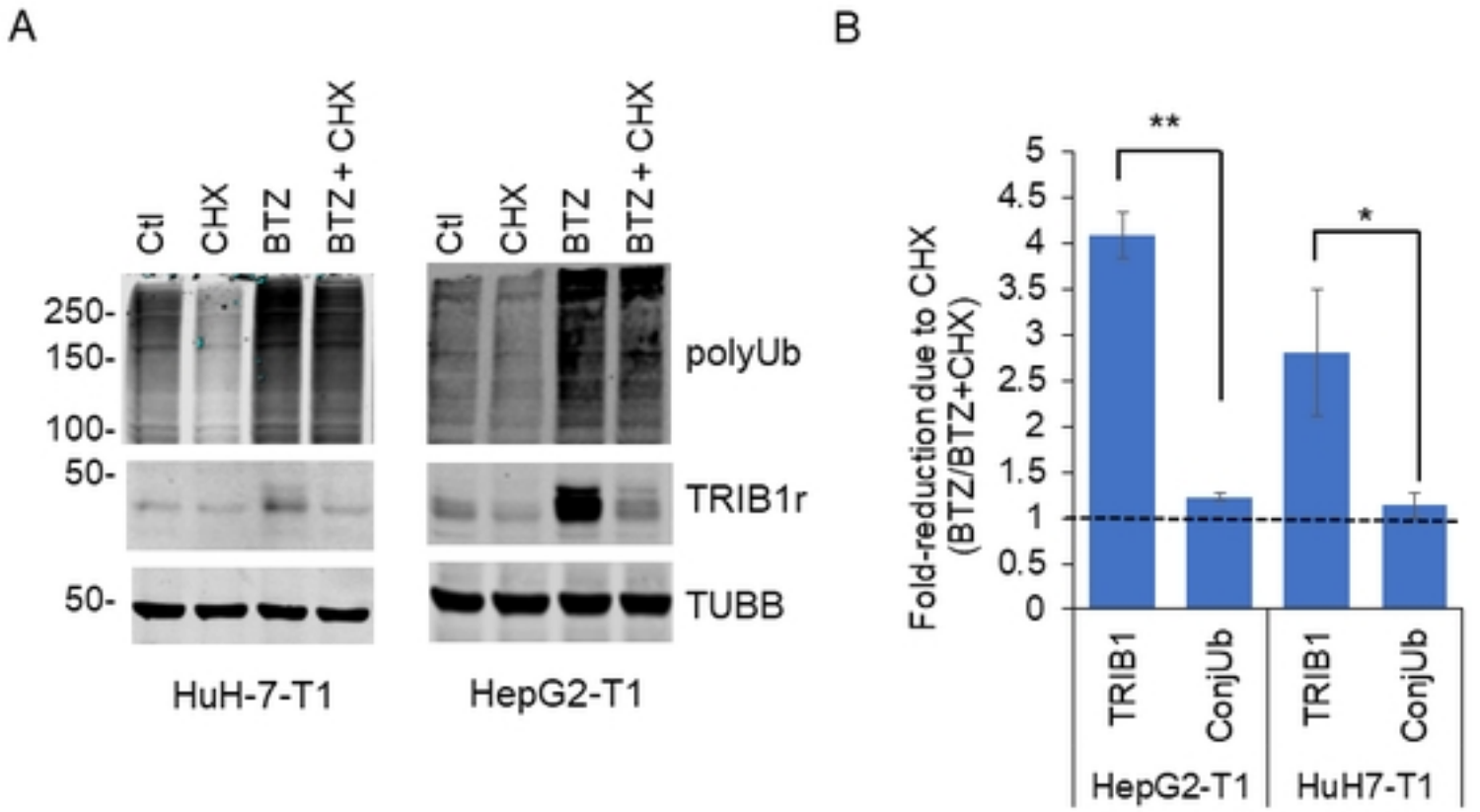
A
Ctl
CHX
BTZ
BTZ + CHX
250-
150-
100-
50-
50-
polyUb
TRIB1r
TUBB
HuH-7-T1
HepG2-T1
B
Fold-reduction due to CHX
(BTZ/BTZ+CHX)
5
4.5
4
3.5
3
2.5
2
1.5
1
0.5
0
**
*
TRIB1
ConjUb
TRIB1
ConjUb
HepG2-T1
HuH7-T1

figure 11

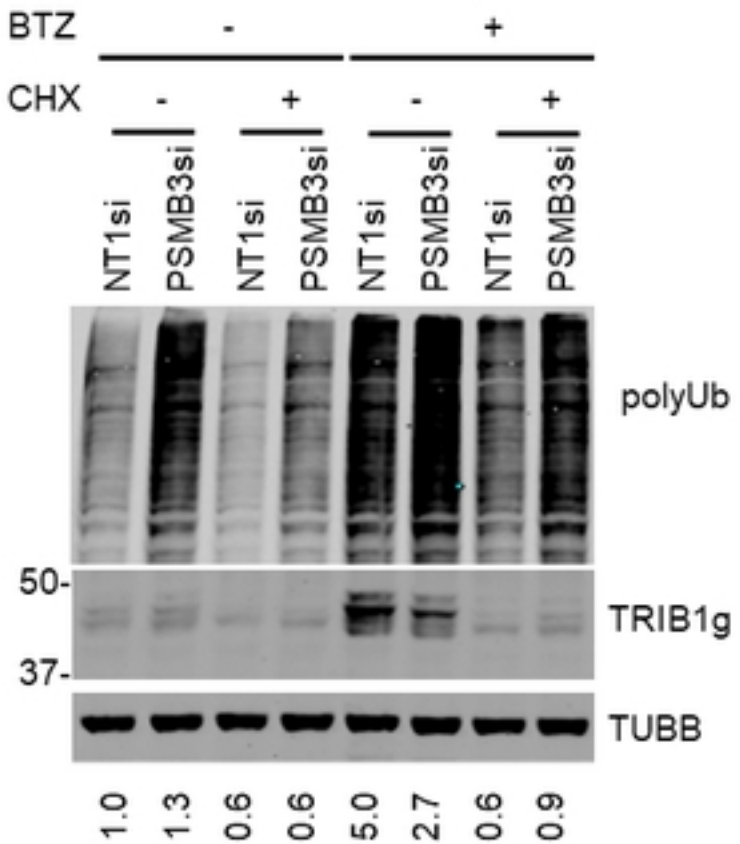
BTZ
-
+
CHX
-
+
-
+
NT1si
PSMB3si
NT1si
PSMB3si
NT1si
PSMB3si
NT1si
PSMB3si
polyUb
50-
37-
TRIB1g
TUBB
1.0
1.3
0.6
0.6
5.0
2.7
0.6
0.9

figure 12

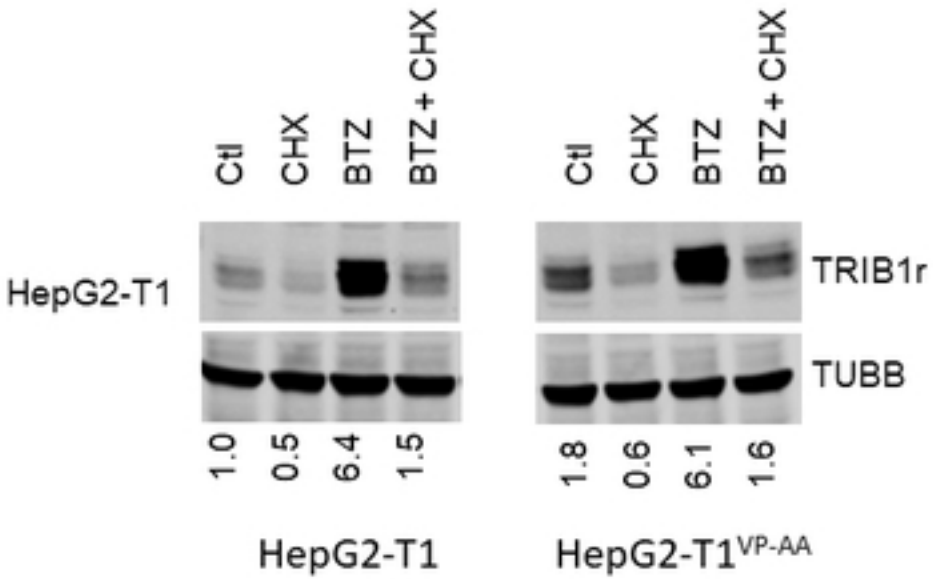
Ctl
CHX
BTZ
BTZ + CHX
Ctl
CHX
BTZ
BTZ + CHX
HepG2-T1
TRIB1r
TUBB
1.0
0.5
6.4
1.5
1.8
0.6
6.1
1.6
HepG2-T1
HepG2-T1VP-AA

figure 13

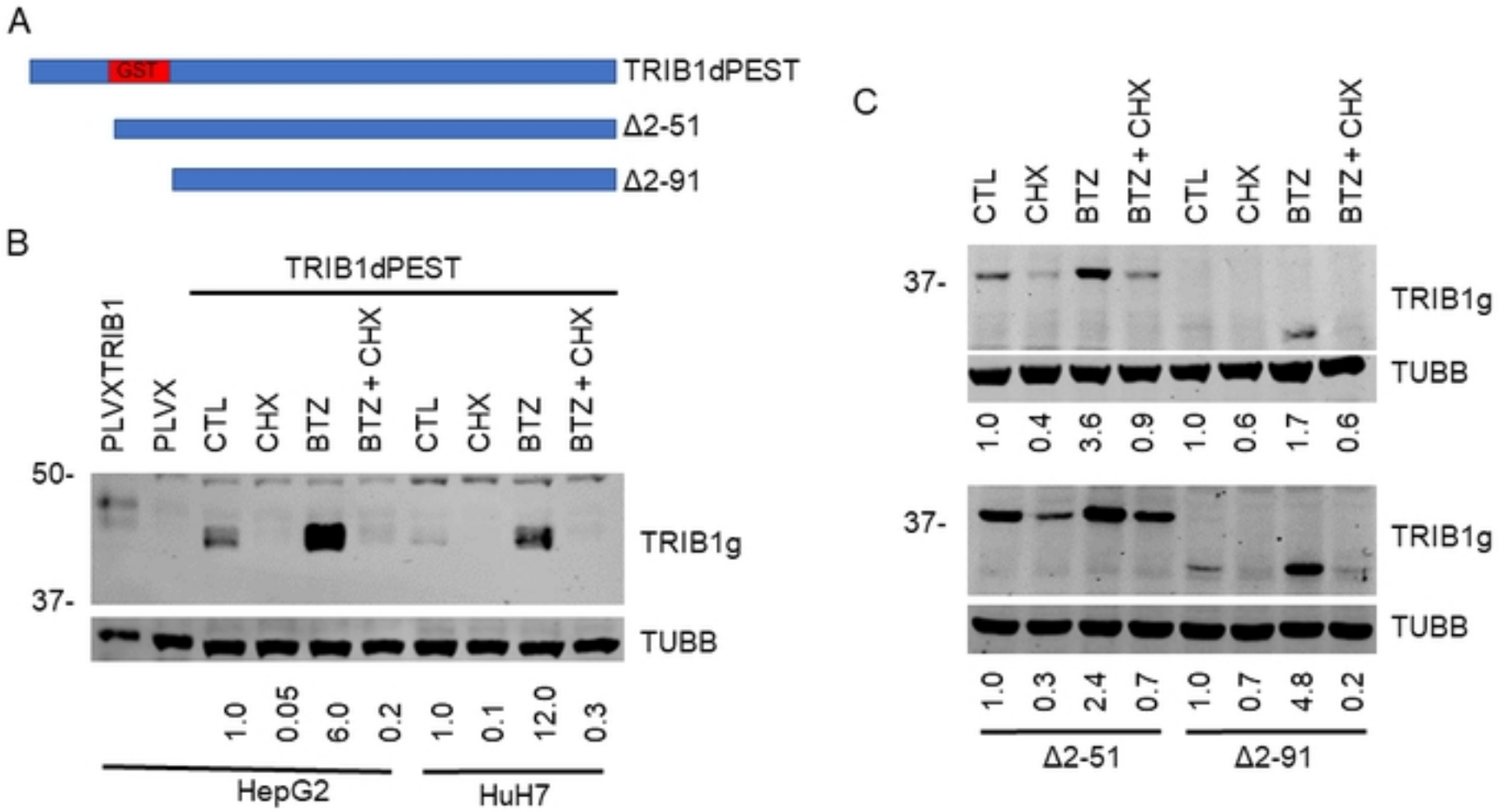
A
GST
TRIB1dPEST
Δ2-51
Δ2-91
B
TRIB1dPEST
PLVXTRIB1
PLVX
CTL
CHX
BTZ
BTZ + CHX
CTL
CHX
BTZ
BTZ + CHX
50-
37-
TRIB1g
TUBB
1.0
0.05
6.0
0.2
1.0
0.1
12.0
0.3
HepG2
HuH7
C
CTL
CHX
BTZ
BTZ + CHX
CTL
CHX
BTZ
BTZ + CHX
37-
TRIB1g
TUBB
1.0
0.4
3.6
0.9
1.0
0.6
1.7
0.6
37-
TRIB1g
TUBB
1.0
0.3
2.4
0.7
1.0
0.7
4.8
0.2
Δ2-51
Δ2-91

figure 14

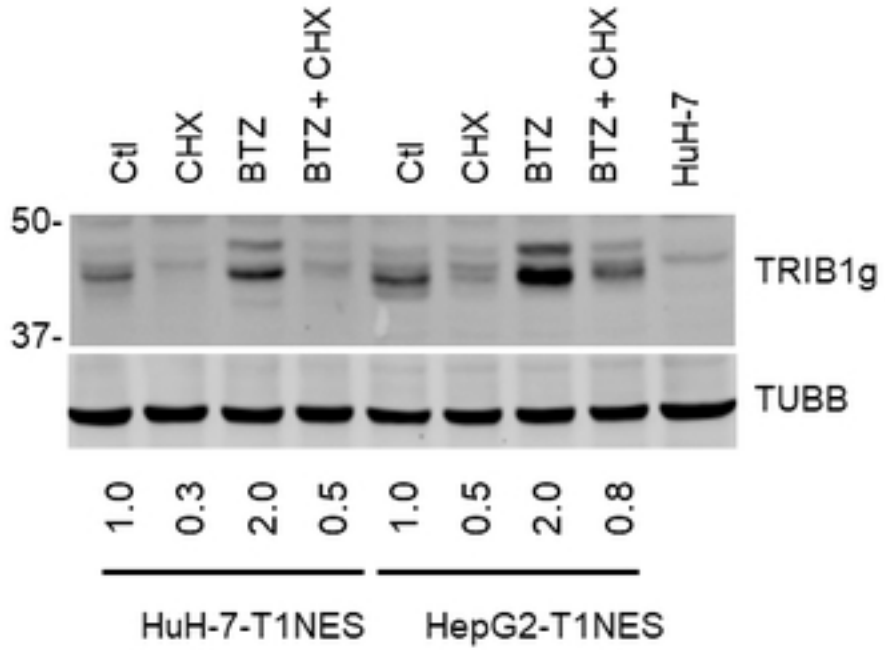
Ctl
CHX
BTZ
BTZ + CHX
Ctl
CHX
BTZ
BTZ + CHX
HuH-7
50-
37-
TRIB1g
TUBB
1.0
0.3
2.0
0.5
1.0
0.5
2.0
0.8
HuH-7-T1NES
HepG2-T1NES

figure 15

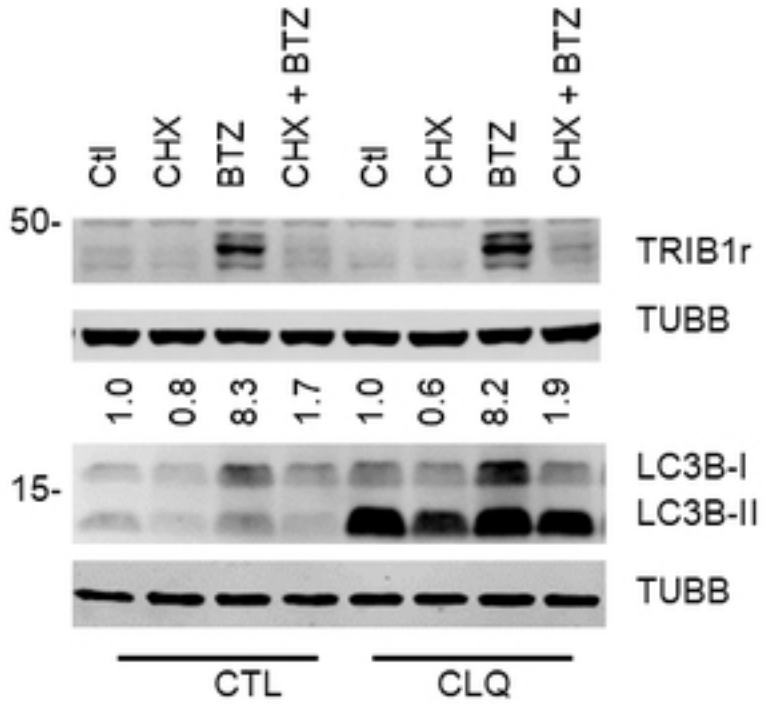
Ctl
CHX
BTZ
CHX + BTZ
Ctl
CHX
BTZ
CHX + BTZ
50-
TRIB1r
TUBB
1.0
0.8
8.3
1.7
1.0
0.6
8.2
1.9
15-
LC3B-I
LC3B-II
TUBB
CTL
CLQ

figure 16

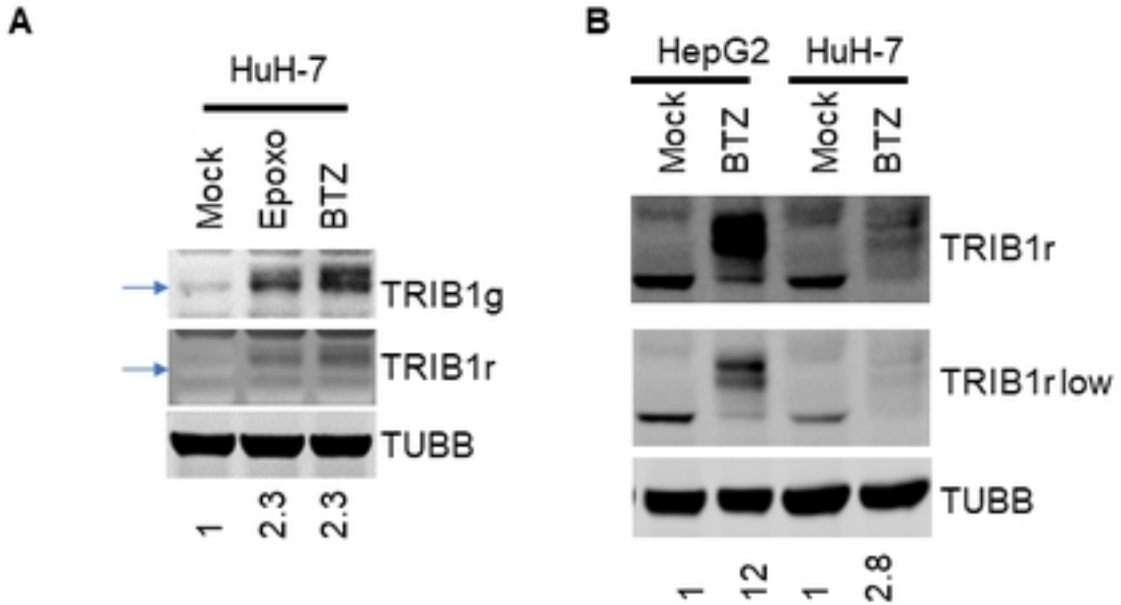
A
HuH-7
Mock
Epoxo
BTZ
TRIB1g
TRIB1r
TUBB
1
2.3
2.3
B
HepG2
HuH-7
Mock
BTZ
Mock
BTZ
TRIB1r
TRIB1r low
TUBB
1
12
1
2.8

figure 2

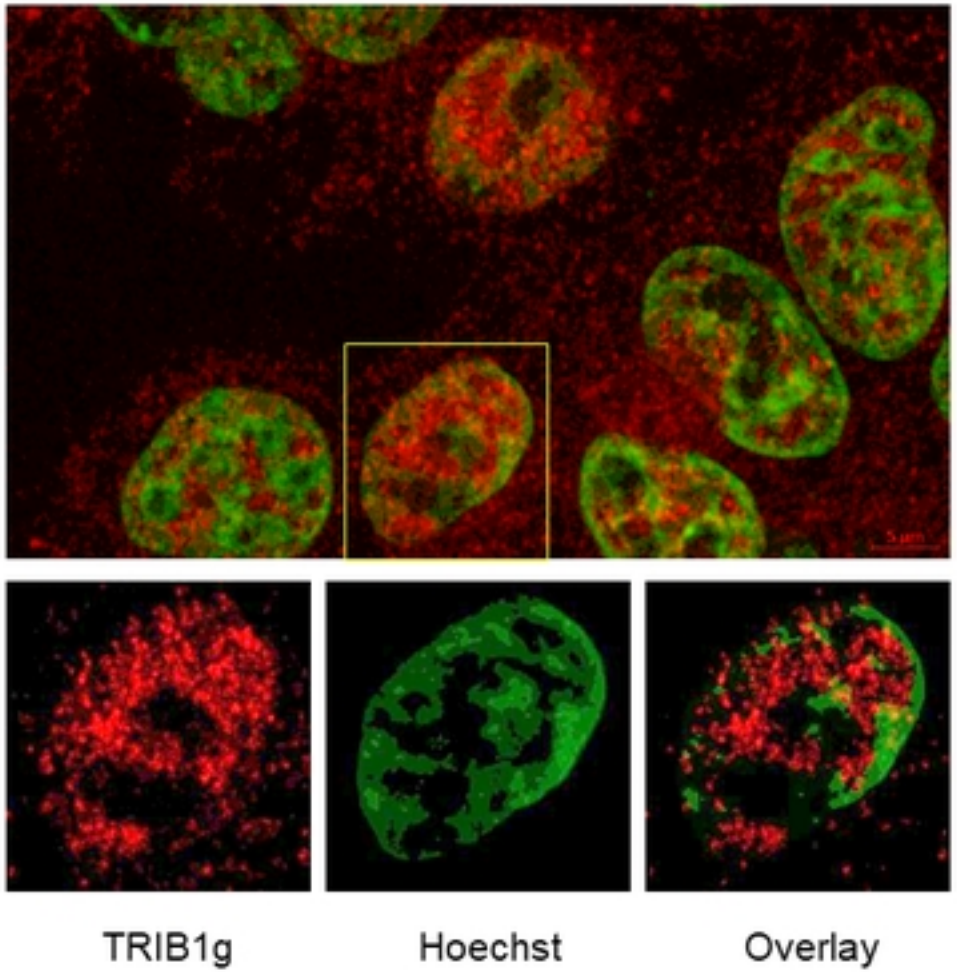


figure 3

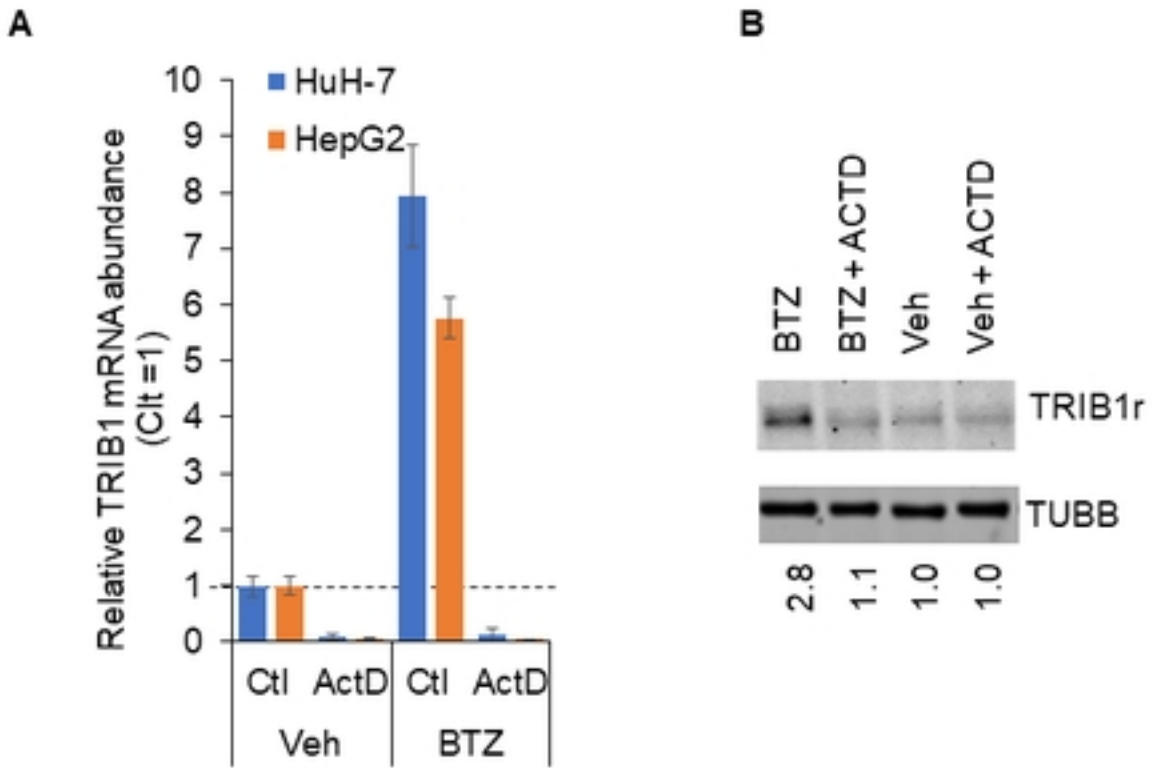
A
HuH-7
HepG2
Relative TRIB1 mRNA abundance (Ctl =1)
10
9
8
7
6
5
4
3
2
1
0
Ctl
ActD
Ctl
ActD
Veh
BTZ
B
BTZ
BTZ + ACTD
Veh
Veh + ACTD
TRIB1r
TUBB
2.8
1.1
1.0
1.0

figure 4

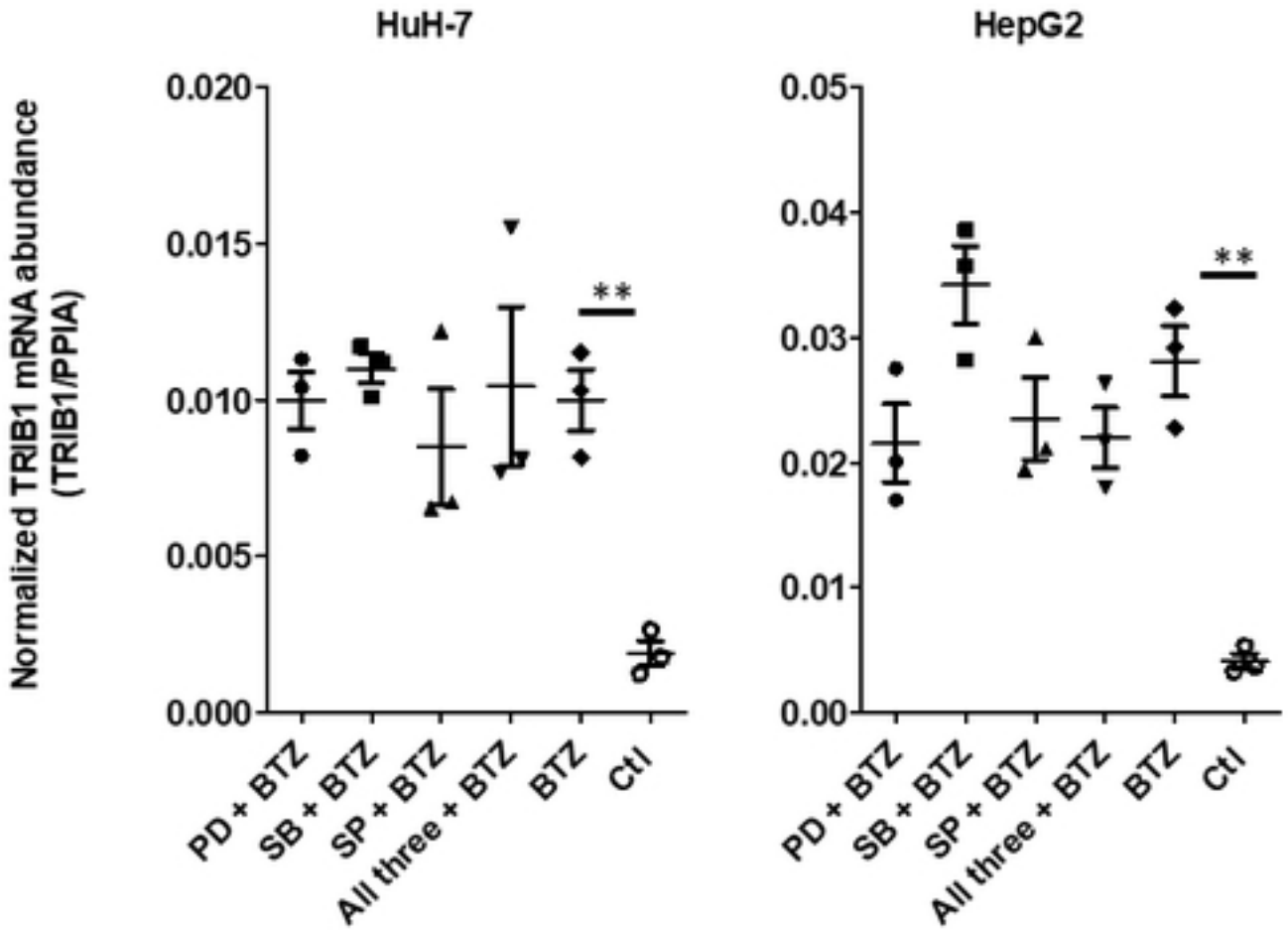
HuH-7
HepG2
Normalized TRIB1 mRNA abundance
(TRIB1/PPIA)
0.020
0.015
0.010
0.005
0.000
0.05
0.04
0.03
0.02
0.01
0.00
**
**
PD + BTZ
SB + BTZ
SP + BTZ
All three + BTZ
BTZ
Ctl

figure 5

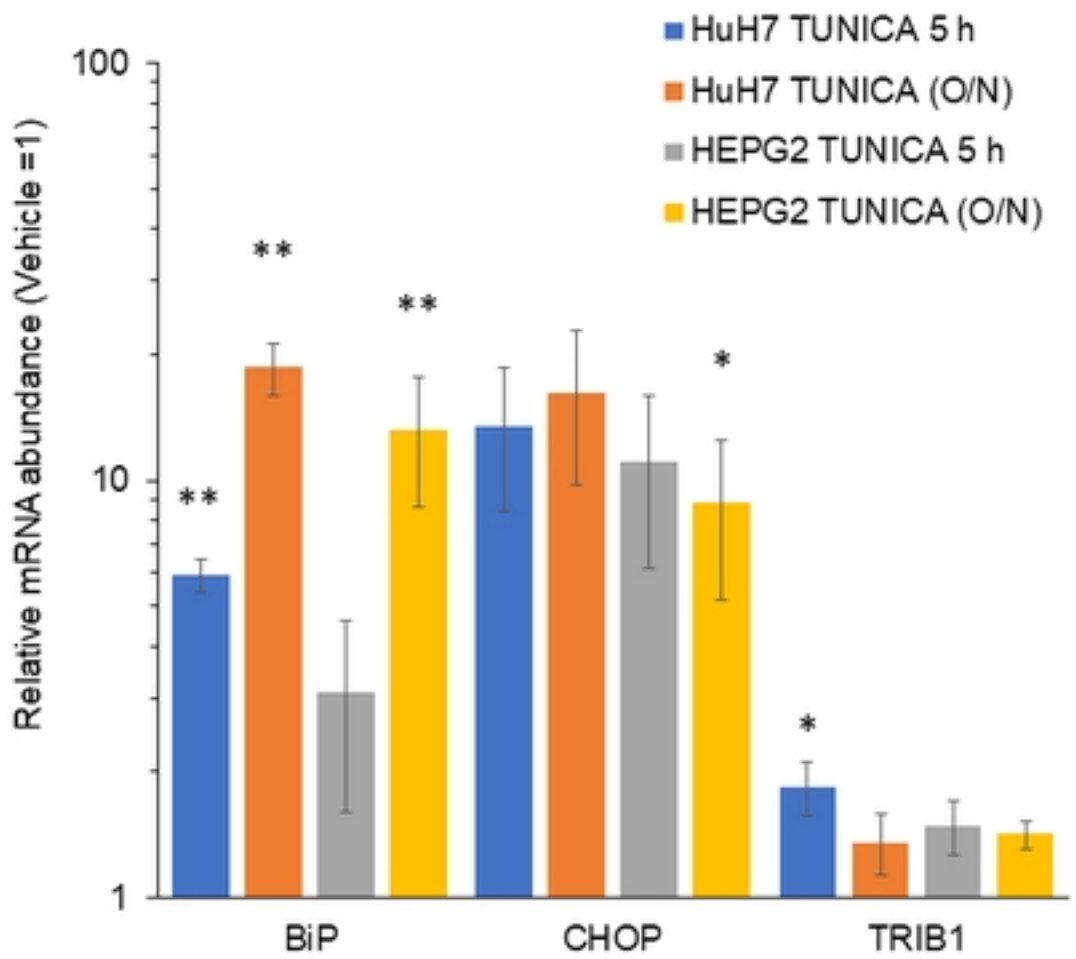
HuH7 TUNICA 5 h
HuH7 TUNICA (O/N)
HEPG2 TUNICA 5 h
HEPG2 TUNICA (O/N)
Relative mRNA abundance (Vehicle =1)
100
10
1
**
**
**
*
*
BiP
CHOP
TRIB1

figure 6

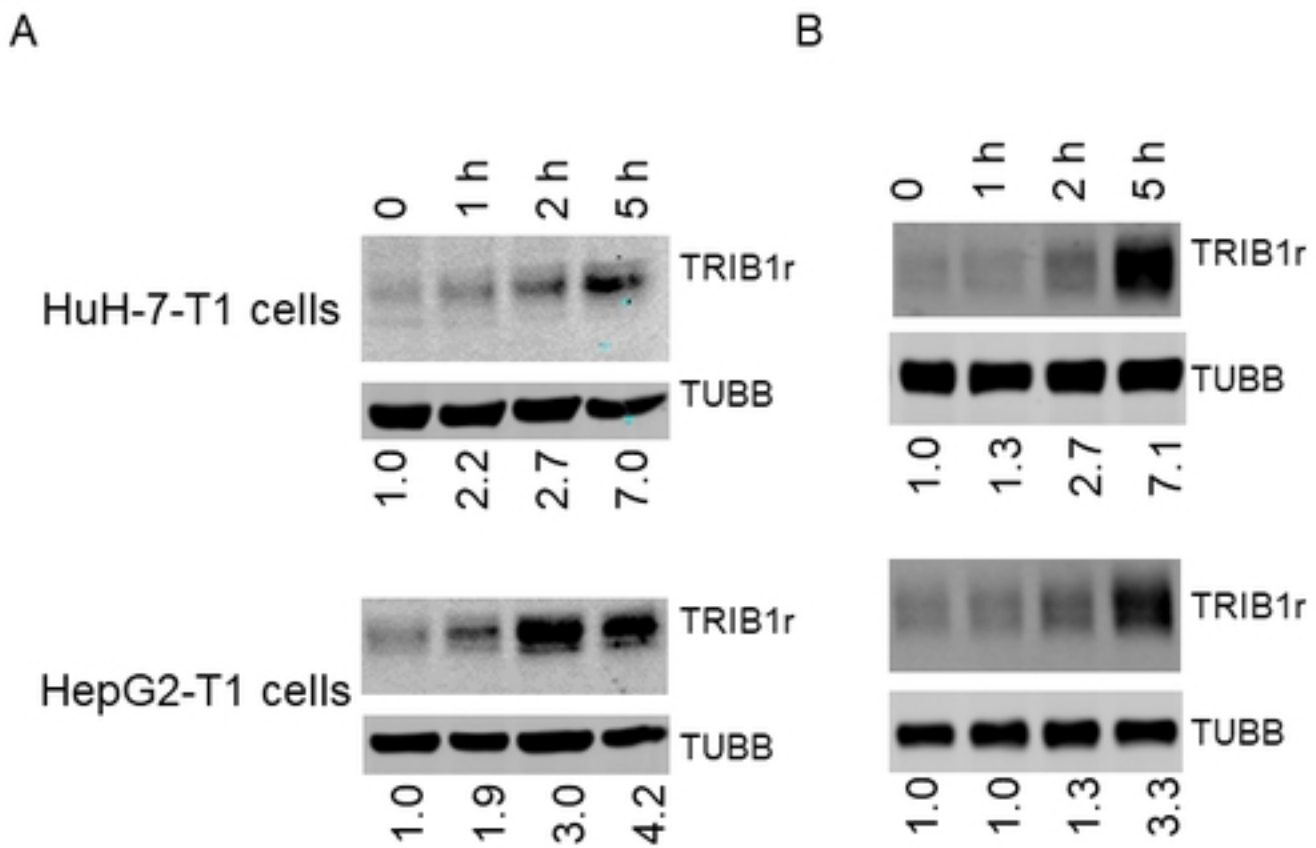
A
B
0
1 h
2 h
5 h
HuH-7-T1 cells
TRIB1r
TUBB
1.0
2.2
2.7
7.0
HepG2-T1 cells
TRIB1r
TUBB
1.0
1.9
3.0
4.2
0
1 h
2 h
5 h
TRIB1r
TUBB
1.0
1.3
2.7
7.1
TRIB1r
TUBB
1.0
1.0
1.3
3.3

figure 7

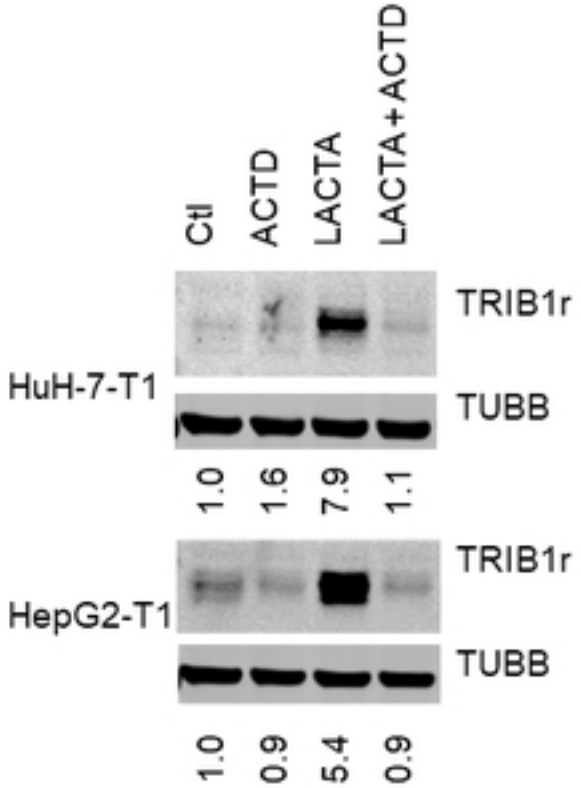
Ctl
ACTD
LACTA
LACTA+ACTD
HuH-7-T1
TRIB1r
TUBB
1.0
1.6
7.9
1.1
HepG2-T1
TRIB1r
TUBB
1.0
0.9
5.4
0.9

figure 8

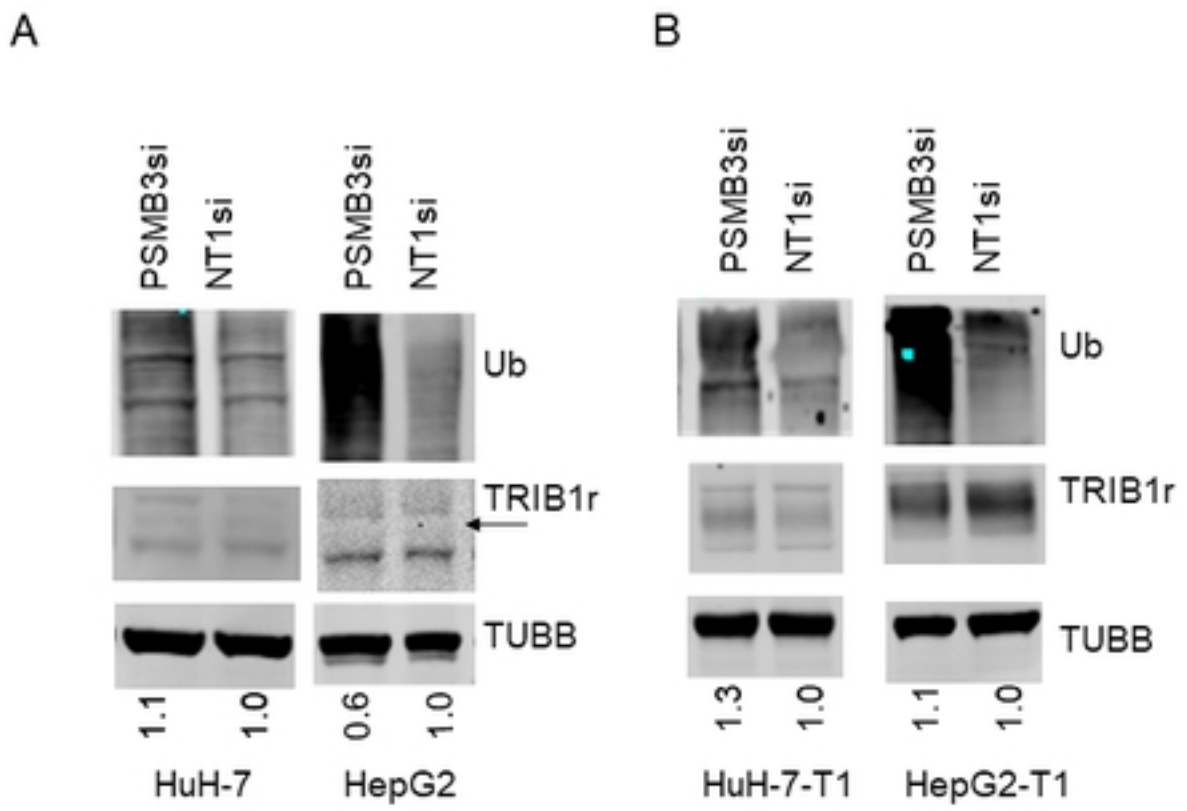
A
B
PSMB3si
NT1si
PSMB3si
NT1si
Ub
TRIB1r
TUBB
1.1
1.0
0.6
1.0
HuH-7
HepG2
PSMB3si
NT1si
PSMB3si
NT1si
Ub
TRIB1r
TUBB
1.3
1.0
1.1
1.0
HuH-7-T1
HepG2-T1

figure 9